Liquid Crystal Domain Formation and Structure in Humic Substances + Water + Hydrocarbon Mixtures

by

Li Lin

A thesis submitted in partial fulfillment of the requirements for the degree of

Master of Science

in

CHEMICAL ENGINEERING

Department of Chemical and Materials Engineering

University of Alberta

Abstract

The liquid crystal phase state has long-range order in one or two dimensions and is an intermediate phase state between the unordered liquid state and the solid crystalline state with long-range order in three dimensions. Liquid crystals, comprising spherical liquid crystalline shells surrounding homogeneous fluid, were first found in water-free petroleum resources and resource fractions in 2010 [1]. From that time, researchers have focused on determining their properties, their fate in industrial production, transport, and refining processes, and their composition [2, 3]. Chemical analysis of liquid crystal enriched samples from Athabasca bitumen suggests that the liquid crystalline material may comprise humic or fulvic acids/salts or humins [4]. In this work, the formation of liquid crystal domains with homogeneous organic or aqueous cores and humic substance-rich liquid crystalline shells dispersed in aqueous or hydrocarbon liquids in hydrocarbon-water emulsions is explored using cross-polarized light microscopy. As liquid crystal domains diffract light, they are typically identified and characterized by light patterns in images arising from passing light through a polarizer, then through the sample, and then through a second orthogonally oriented polarizer. For these cases, a Maltese cross pattern is expected. As artifacts arise with this methodology, care must be taken to eliminate or mitigate them through baseline measurements, control experiments, and calibration. So far, processes leading to the formation of liquid crystal-rich domains with organic cores/ aqueous cores and humic substance-rich liquid crystalline shells dispersed in aqueous solutions and aqueous cores with humic substance-rich liquid crystalline shells dispersed in organic solutions have been demonstrated. Formation processes leading to these domains dispersed in hydrocarbon liquids, have yet to be identified. Although more

researches are needed, the results contribute to the understanding of hydrocarbon resources' properties and the development of improved separation and refining processes for hydrocarbon resources.

Acknowledgement

First and foremost, a sincere gratitude goes to my supervisor Dr. John Shaw. Thanks for your inspiring talks and guidance. No matter when I got stuck during my experiments, I could always get new ideas and directions after discussing with you. Thanks for your patience and numerous encouragements. I was experiencing a negative period and you always encouraged me and never gave me up.

Thanks to Dr. William McCaffrey and Dr. Hongbo Zeng from the University of Alberta for allowing me to use their laboratories and equipments.

I would also thank Mr. Kejie Wang and Ms. Mildred Becerra for equipment training and technical instructions at the initial stage of my project. Thanks to Mr. Cedric Laborade-Boutet for helping set up the Hot Stage Microscope and Dr. Yanbin for instructing the use of Zetasizer Nano unit. The support of my colleagues from the Petroleum Thermodynamic Group is also important. I thank Mr. Sourbh Ahitan and Mr. Sahil Sood, especially, for their nice discussions when I encountered questions during my experiments.

Last but not least, I thank my parents and my brother, for their endless love and support throughout my whole life. Thanks Jingjing Ji for her love and encouragement.

Table of Contents

List of Figures

List of Tables

Nomenclature

HA	Humic acid
SAGD	Steam Assisted Gravity Drainage
r	Static Fluorescence Anisotropy
FTIR	Fourier Transform Infrared Spectroscopy
FT-ICR	Fourier Transform Ion Cyclotron Resonance
CMC	Critical Micelle Concentration
LSLHA	Lathhco Silt Loam Humic Acid
LHA	Humic Acid with Lignite Deposits
SRHA	Ritzville Soil Humic Acid
RSHA	Humic Acid Extracted from Ritzville soil
PLVHA	Humic Acid Extracted from Pilayella Littoralis
EHA	Ethanol Extracted Humic acid
5 CB	4′-Pentyl-4-biphenylcarbonitril
PLM	Polarized Light Microscope
HSM	Hot Stage Microscope
OTS	Octadecyltrichlorosilan

Chapter 1. Introduction

The liquid crystal state is an intermediate phase state that exhibits long-range order in one or two-dimensions between the isotropic liquid state and the crystalline solid state that exhibits three-dimensional order. Liquid crystals may flow like liquids [5] and share properties with both solids and liquids. Liquid crystals have been widely studied because of their optical and electrical anisotropic characteristics and magnetic properties [5]. Liquid crystals can also be amphiphilic and contribute to the stabilization of emulsions and dispersions by hindering coalescence, flocculation, and phase separation [6-8]. For example, liquid crystals can be located at interfaces in oil-water emulsions [7, 9-13].

Liquid crystals were first observed in petroleum in 2010 [1]. These liquid crystals, pictured in Figure 1-1, are biplex [14]. They comprise a thin liquid crystal shell surrounding a homogeneous hydrocarbon liquid core. They exhibit thermotropic and lyotropic behaviors,i.e., and they appear or disappear as a function of global composition at a fixed temperature and arise over a fixed temperature range. This discovery launched a series of studies [2-4] intended to isolate and identify these materials chemically and to discriminate impacts of these species and asphaltenes – another fraction of crude oils. Interfacial stability and surface deposition problems arising in the petroleum production, transport, and refining industries have been attributed to asphaltenes, including the stabilization of w/o emulsions [15]. The origin of some of these problems might be misattributed.

While the resolution of some behaviors of liquid crystalline materials has proven feasible, such as their fate in surface facilities associated with SAGD (Steam Assisted Gravity Drainage) processes [3], isolation and analysis of liquid crystals from petroleum have proven to be challenging [4,14].

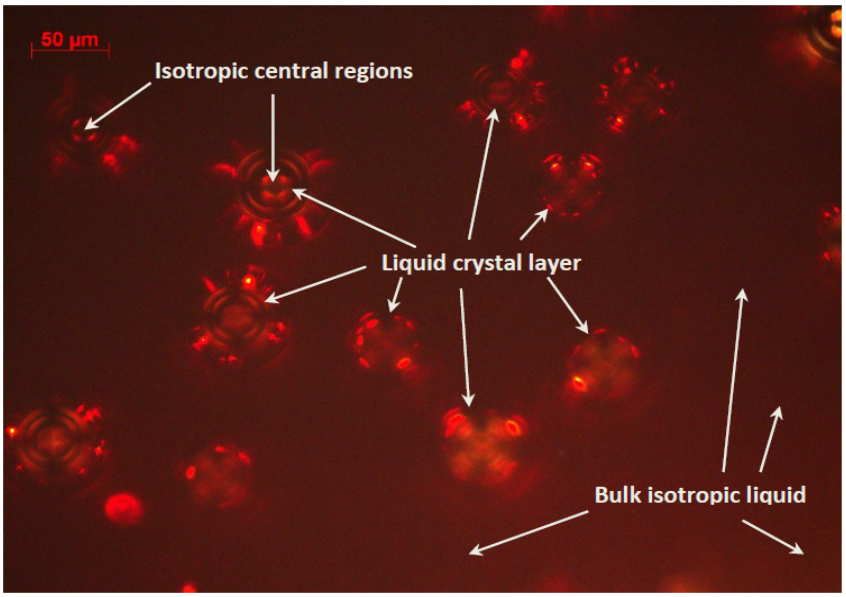

Figure 1-1 Liquid crystals observed in C_5 maltenes. The liquid crystals that include an isotropic central region are suspended in a bulk isotropic liquid [14].

The latest research indicates that these liquid crystals appear to comprise humic substances, including humic and fulvic acids [4]. These materials are known to exhibit fluorescence anisotropic properties in aqueous solution [16] and are present in ore of oil sands [17]. Humic substances are produced by biodegradation of organic matters and are the components of humus. The compounds found in humic substances possess high molar masses and are enriched in oxygen-containing functional groups such as hydroxyl and carboxyl groups [18]. Based on the difference of solubility of each fraction in

aqueous media, humic substances can be subdivided into humic acids (HA), fulvic acids (FA), and humins. Humic acids are dark-colored organics that can be extracted from aqueous solution at low pH.

The research reported in this thesis focuses on possible liquid crystal phase behaviors of humic acids in water + hydrocarbon mixtures. It is intended to test the hypothesis that humic acids exhibit the properties of liquid crystals observed in crude oils and crude oil fractions. The formation of four types of biplex liquid crystals comprising liquid crystal humic acid-rich shells and isotropic hydrocarbon and aqueous phases is targeted (Figure 1-2). The key research question is whether it is possible to prepare the four prototype liquid crystal objects.

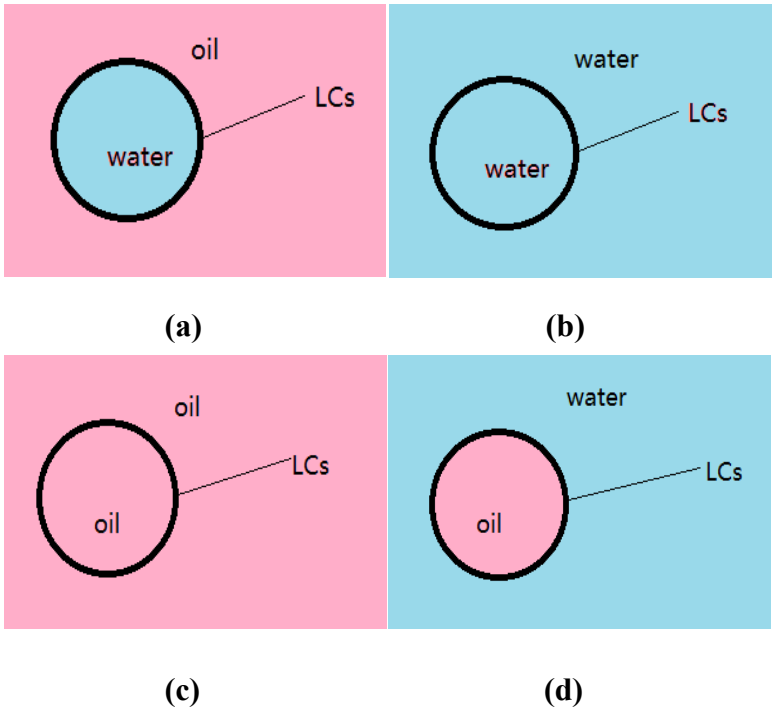

Figure 1-2 Four possible formations of humic acid liquid crystal layers at hydrocarbon-water interface.

This thesis is divided into five chapters including the introduction (Chapter 1). Chapter 2 comprises literature reviews on topics related to liquid crystals, liquid crystals in petroleum and humic acids, and on the formation of multiphase drops at liquid-liquid interfaces. Chapter 3 describes the experimental methods used in this work. Chapter 4 presents the experimental results obtained and their discussion. Chapter 5 presents the conclusions and recommendations for future work.

Chapter 2. Literature Review

2.1 Liquid Crystals

Matter possesses three classic states: liquid, solid, and gas. Crystalline solids possess three-dimensional long-range order or display orientational order. Isotropic liquids present neither positional nor orientational long-range order [19]. Liquid crystals are an intermediate state possessing either one-dimensional or two-dimensional long-range order. They can flow like isotropic fluids and yet have the anisotropic optical properties associated with solid crystals. Liquid crystals can be classified as thermotropic, lyotropic, and amphotropic based on the field variables that induce phase transitions to liquid crystals [19]. For thermotropic liquid crystals, temperature and pressure are the field variables. An illustrative schematic is shown in Figure 2-1 [20]. For lyotropic liquid crystals, transitions are driven by changes in composition at a fixed temperature [5]. The basic units of lyotropic liquid crystals are supermolecular structures produced from the self-assembly of amphiphilic molecules [19]. For most lyotropic mixtures, water is present [21]. Liquid crystals showing both lyotropic and thermotropic properties are classified as amphotropic. An example of lyortopic liquid crystal structure is shown in Figure 2-2 [22].

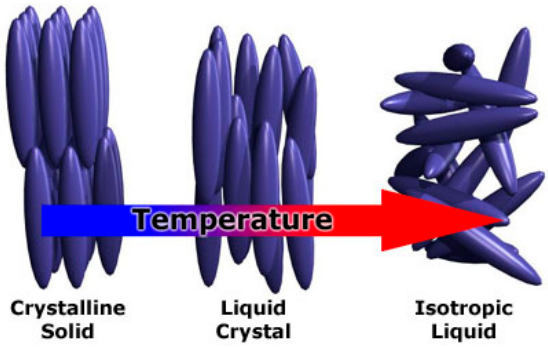

Figure 2-1 A schematic showing the phase transition of thermotropic liquid crystals [20].

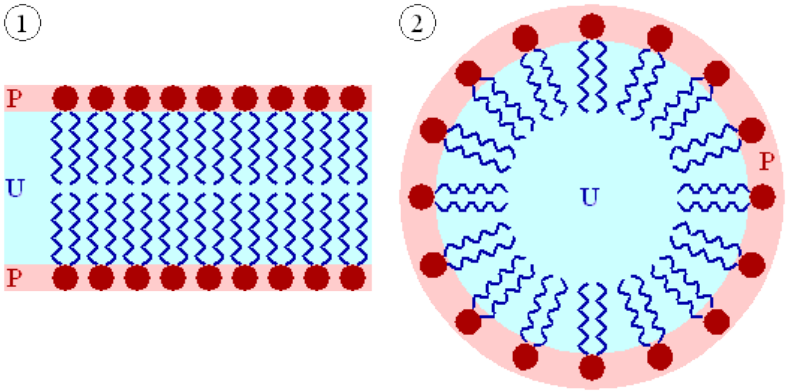

Figure 2-2 Structure of lyotropic liquid crystal. The redheads of surfactant molecules are in contact with water, whereas the tails are immersed in oil (blue): bilayer (left) and micelle (right) [22].

Depending on the alignment features, there are three common physical structures of liquid crystals [23, 24]: nematic liquid crystals, sematic liquid crystals, and columnar liquid crystals. In nematic liquid crystals, molecules tend to align in a certain direction but have no positional order. Sematic liquid crystals present a degree of translational

order because the molecules tend to align in layers or planes. For columnar liquid crystals, the molecules assemble in two dimensions and form the discotic columns, showing long-range order in two dimensions. These features are illustrated in Figure 2-3 [25].

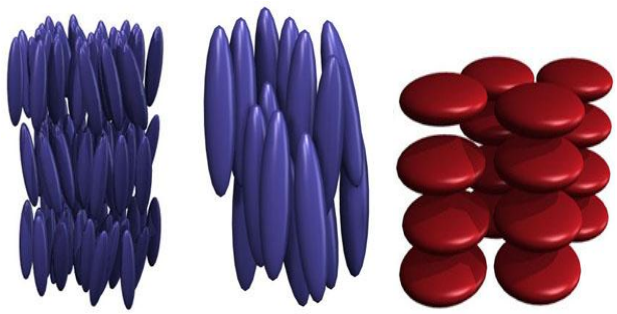

Figure 2-3 Left: smectic liquid crystals; middle: nematic liquid crystals; right: columnar liquid crystals [25].

2.2 Polarized Light Microscopy

2.2.1 Background

Polarized light microscopy is a convenient technique to observe and image anisotropic materials like liquid crystals. Microscopes equipped with two polarizing lenses set orthogonally are used. The first polarizer is positioned in the light path and ahead of the specimen, while the second one is placed beyond the specimen and is orthogonal to the first lens [26]. If the specimen is isotropic, the polarized light is blocked by the second lens and the specimen appears dark to an observer positioned further along the light path. If the specimen is anisotropic, the direction of the polarized light is altered, and a fraction of it passes through the second lens and shows an optical pattern [26]. Figure 2-4 illustrates the principles of the polarization of light waves. Different types of liquid

crystals show different optical patterns, including Maltese cross patterns, fan-shaped patterns, and other patterns (Figure 2-5) [27, 28]. Researchers have assigned the appearance of Maltese crosses in images obtained in polarized light microscopy as evidence of the emergence of liquid crystals in previous works. Liquid crystals observed in some heavy oils show Maltese crosses [4, 15, 29]. Figure 2-6 shows an example of a Maltese cross pattern under polarized light formed by liquid crystal observed in C_5 asphaltenes [14].

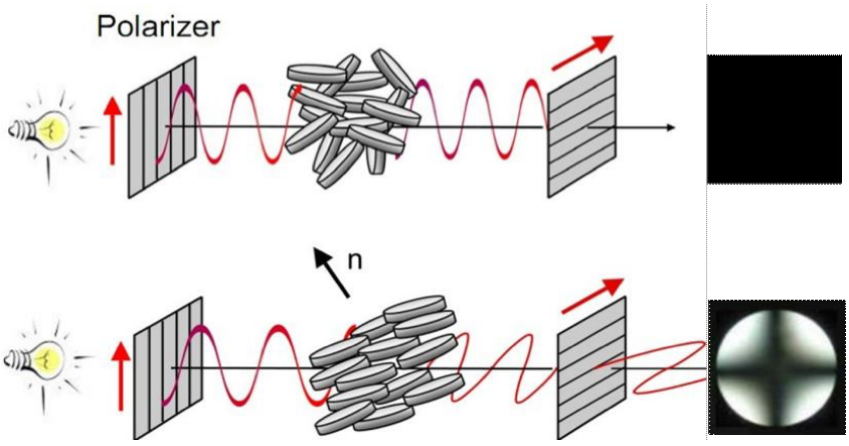

Figure 2-4 A schematic of the polarized light microscope (top: isotropic material under cross-polarized light; bottom: anisotropic material under cross-polarized light) [29].

Figure 2-5 Liquid crystals patterns under polarized light: (a) fan-shaped pattern formed by 4′ -Pentyl-4-biphenylcarbonitrile droplets sitting on the hydrophilic glass; (b) Maltese cross pattern formed by 4-Pentyl-4-biphenylcarbonitrile droplets sitting on the hydrophobic glass; [27] (c) other patterns formed during phase transition between a nematic (left) and smectic A (right) phases [28].

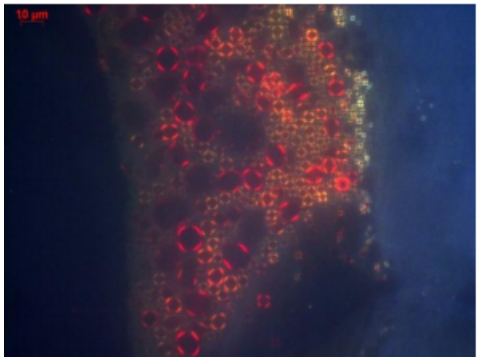

Figure 2-6 Enriched liquid crystals extracted from C_5 asphaltenes [14].

2.2.2 Artifacts

When working with emulsions, caution is needed to interpret light patterns associated with the emergence of liquid crystals. According to Rayleigh's classical scattering law, an initially unpolarized light beam becomes polarized when scattered [30]. As oil-water interfaces can scatter and polarize incident light, they can show a light intensity region with an apparent thickness that produces a false impression that liquid crystals are present [31]. Figure 2-7 shows an example of oil emulsion droplets in the water showing Maltese cross artifact under polarized light [33]. The refractive index difference between the oil and water phases [31], the curvature of optical surfaces [32], and light interference among multiple drops in bulk liquid contribute to this artifact. Care must be taken, as was done in this work, to avoid misinterpretation of experimental outcomes.

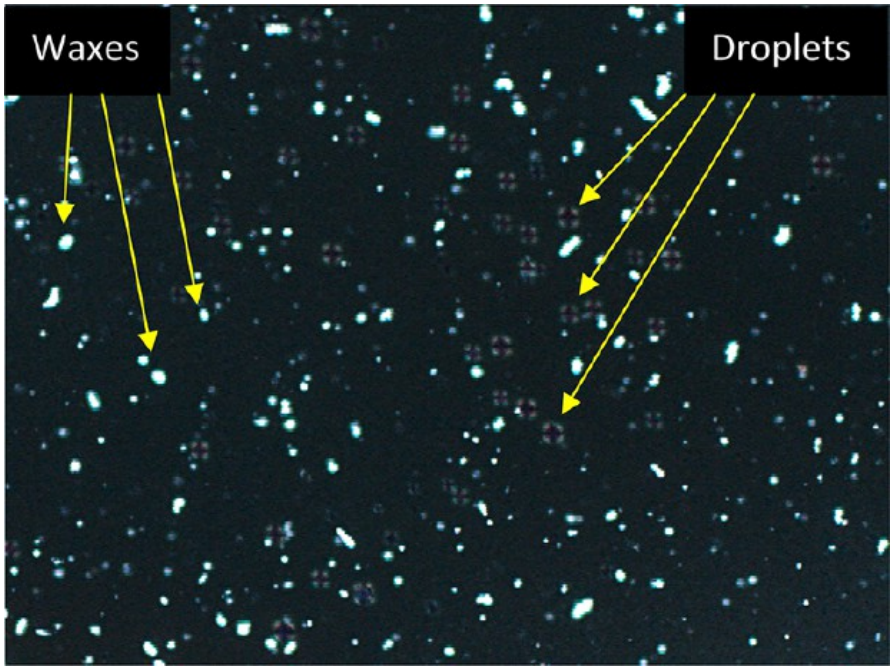

Figure 2-7 Crude oil emulsion drops in the water showing a Maltese cross repolarization artifact [33].

2.3 Liquid Crystals in Petroleum

2.3.1 Physical Properties

That the observation of liquid crystal in petroleum has contributed to a better understanding of the phase behavior and interfacial properties of unreacted petroleum fractions, including Maya and Cold Lake pentane asphaltenes, Athabasca, and Safaniya heptane asphaltenes. Although the liquid crystals observed in these asphaltenes present different phase transition temperature ranges, all exhibit both thermotropic and lyotropic phase transitions, and are thus defined as amphotropic liquid crystals [1]. These liquid crystals also transfer from bitumen-rich to water-rich phases both in laboratory measurements and industrial SAGD facilities [29]. Liquid crystal domains are observed

at oil-water interfaces [31,32] and water-in-crude oil emulsions [33] and have been shown to help stabilize emulsions.

2.3.2 Composition of Liquid Crystals in Heavy Oil

Masik [14] developed an approach to isolate liquid crystal enriched samples from bitumen by solvent extraction. After analyzing the isolated liquid crystal enriched material from Athabasca asphaltenes by Fourier Transform Ion Cyclotron Resonance Mass Spectrum (FT-ICR-MS), it was found that the molecular mass of liquid crystal material was lower and the mass range was narrower (Figure 2-8) than that of the parent bitumen sample. Figure 2-9 and Figure 2-10 display the heteroatom classes of enriched liquid crystals and Athabasca C_7 asphaltenes respectively. [14] The results show that the liquid crystal enriched sample present higher relative abundances of nitrogen, oxygen, and sulfur than asphaltenes.

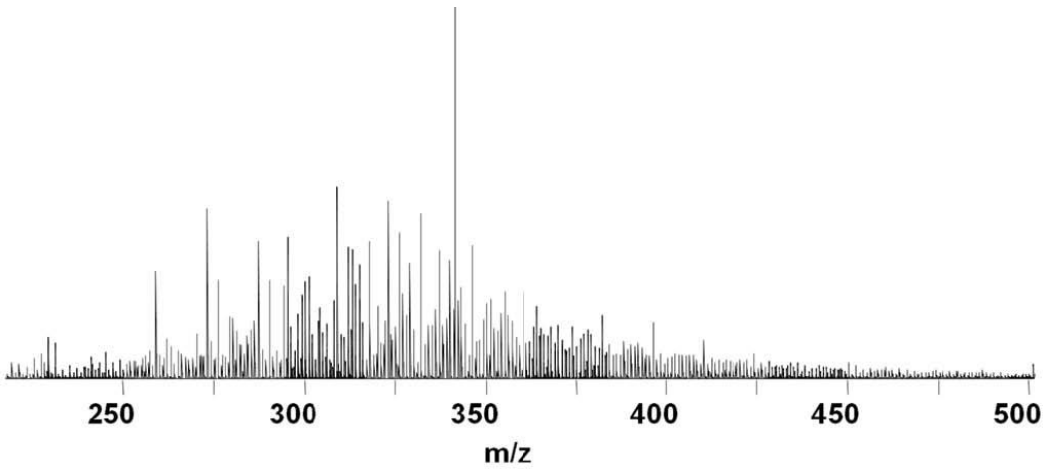

Figure 2-8 Mass spectrum of a liquid crystal enriched sample [14].

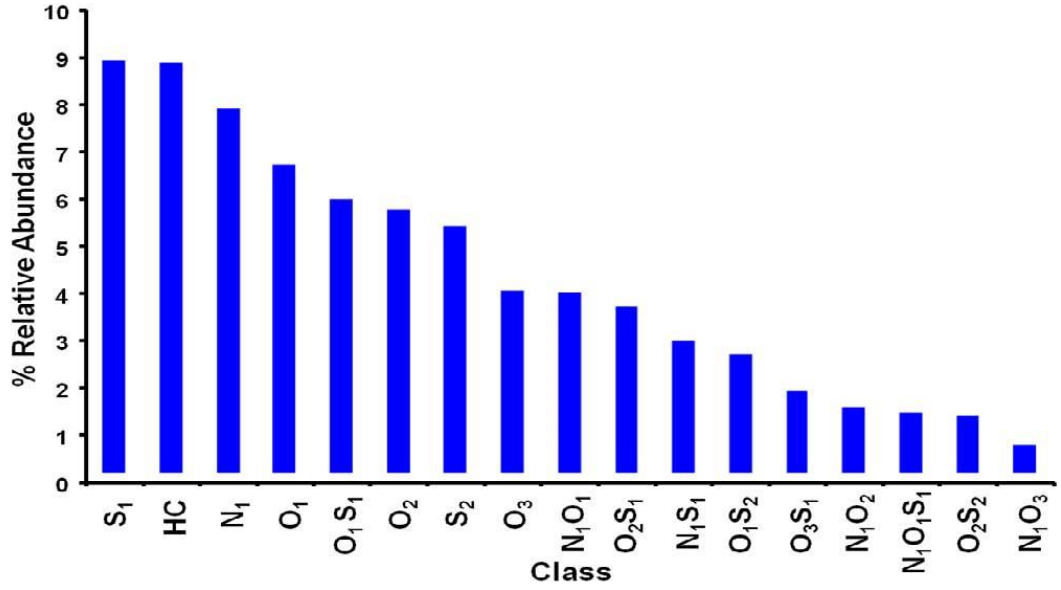

Figure 2-9 Heteroatom abundance distribution for a liquid crystal enriched sample derived from Athabasca C_5 asphaltenes [14].

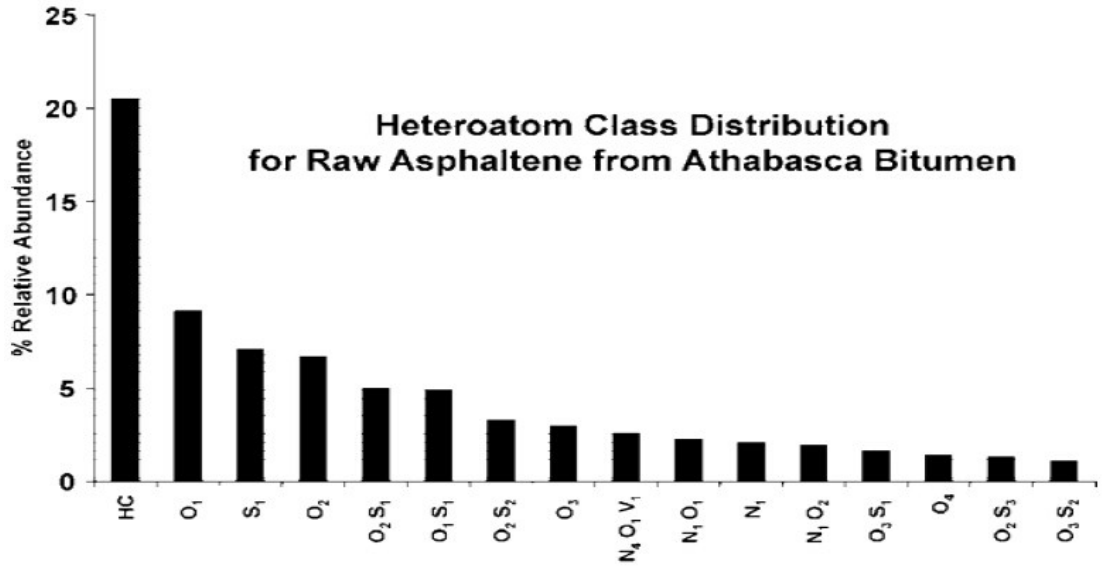

Figure 2-10 Heteroatom abundance distribution for Athabasca C_7 asphaltenes [14].

Kejie Wang [4] implemented physical and chemical separation methods to isolate liquid crystal-rich material from SAGD produced water and analyzed the samples by elemental analysis, and negative-ion Electrospray Ionization sourced Fourier Transform Ion Cyclotron Resonance Mass Spectrometry (FT-ICR MS). The physical isolation method

was based on the coffee ring effect. Liquid crystals in a drop tend to migrate to the edge area as the drop evaporates where they form a ring [29]. The material taken from the rim area is expected to be rich of liquid crystals. The results of physical separation were not as successful as expected. The chemical separation was then implemented by adjusting the pH values of the bulk. At a pH of 3.3, samples separated into two layers [4]. A fraction of the liquid crystals were suspended in the upper layer, while bitumen, clay, and mineral particles remained in the lower layer [4]. Table 2-1 listed the samples and their origins.

Table 2-1 A brief description of the five samples analyzed in Kejie Wang's work [4]

Preparation	Sample name	Sample description
"Froth treatment" and Distillation treatment	Sample 1	Processed water sample
Chemical Deposition of Sample 1	Sample 2	LC-rich sample with little interference from bitumen
	Sample 3	LC-rich sample mixed with bitumen
Coffee Ring Effect of Sample 1	Sample 4	Edge area sample
	Sample 5	Central area sample

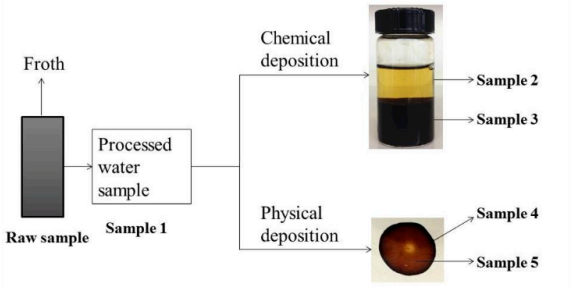

As it is shown in Table 2-1, Sample 2 present the highest relative composition of liquid crystal-rich material, and contained high abundances of carboxylic acids (-COOH), oxyacids and other oxygen-rich species [4]. From mass-based analyses of humic and fulvic acids, reported by Rice and MacCarthy [35], humic substances are the most

probable candidates for the liquid crystal fraction of Athabasca bitumen [4]. The ranges of atomic ratios of sample 2, bitumen, and liquid crystal constituent candidates are listed in Table 2-2.

Table 2-2 Atomic ratios of samples, bitumen and candidate species, reprinted from [4]

	C	H	O	N	S
Sample 2	1	2.09 ± 0.37	0.83 ± 0.08	0.02 ± 0.02	0.06 ± 0.03
Bitumen [36, 37]	1	1.400	0.015	0.004	0.024
Naphthenic acid [38]	1	1.40-2.00	0.10-0.20	0	0
Humic acids [39]	1	0.08-1.85	0.08-1.20	0.05	0.01
Fulvic acids [39]	1	0.77-2.13	0.17-0.19	0.04	0.01
Humin [39]	1	0.82-1.72	0.37-0.61	0.06	0.00
Polysaccharides [40] $(C_6H_{10}O_5)n$	1	1.7	0.83	0	0

2.4 Humic Acids

2.4.1 General Introduction of Humic Acids

Figure 2-11 Solids of humic acids.

Humic substances are a category of naturally occurring materials resulting from the decomposition of plants and animal residues. They can be extracted from soils, natural waters, sediments [40] and oil sand ores [41]. Humic substances are classified into three main fractions: humic acids (HA), fulvic acids (FA), and humins. Humic acids are soluble in water under alkaline conditions, but not soluble under acidic conditions [40]. They have hydrophobic and hydrophilic segments [18] and are classified as amphiphilic. They are dark-coloured powders and have a molar mass between 3,000 and 10,000 g/mol [18]. The solids of humic acids are shown in Figure 2-11. It is difficult to obtain the accurate structural formulas of humic substances because of the large number of components associated with the numerous binding linkages. However, each fraction of humic substances (humic acids, fulvic acids and humins) can be regarded as a family of molecules with differing sizes, having the same structural configuration or functional groups [42]. The essential functional groups are listed in Table 2-3, and Figure 2-12 shows an example of a typical humic acid molecule.

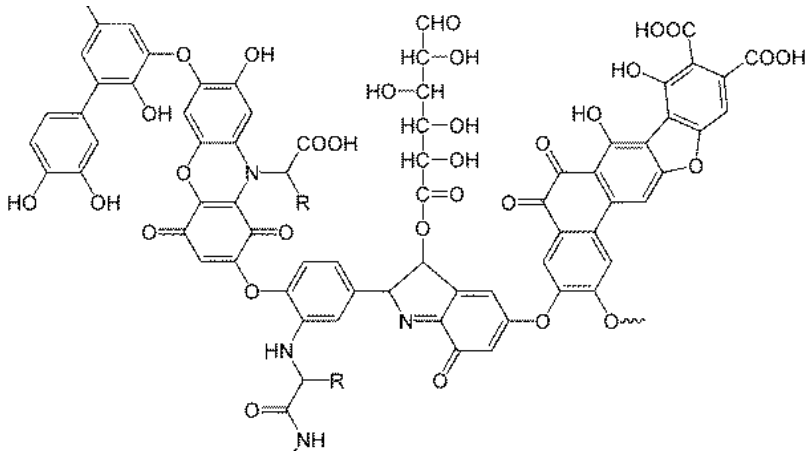

Figure 2-12 An example humic acid molecule [42].

Table 2-3 Important functional groups in humic acids [41].

	Functional Group	Structure
Acidic Groups	Carboxylic	R-C=O(-OH)
	Enaol	R-CH=CH-OH
	Phnenolic OH	Ar-OH
	Quinine	Ar=O
	Alcoholic OH	$R-CH_2-OH$
	Ether	$R-CH_2-O-CH_2-R$
Neutral Groups	Ketone	R-C=O(-R)
	Aldehyde	R-C=O(-H)
	Ester	R-C=O(-OR)
Basic Groups	Amine	$R-CH_2-NH_2$
	Amide	R-C=O(-NH-R)

2.4.2 Micelle formation and its anisotropic properties of Humic Acid solutions

Humic acids can form micelles because they possess both hydrophobic and hydrophilic function groups [43]. Above the critical micelle concentration (CMC), the hydrophobic portions of the molecules associate with one another to form hydrophobic cores, leaving the hydrophilic functional groups oriented out into the bulk aqueous environment [44]. Lyotropic liquid crystals can be formed if the concentration of amphiphilic molecules is higher than the CMC value [45]. Young and Wandruszka [16] tested the fluorescence anisotropy values of HA solutions in glycerol and suggested that pseudomicelle formation took place. In fluorescence anisotropy spectroscopy, the exciting radiation and the emission are passed through polarizers. The value of static fluorescence anisotropy *r* is a measure of the rotational diffusion in a solution. $r = 0$ means the emission is completely depolarized by the solution and the maximum value of *r*, corresponding to the occasion that no process of depolarization occurs, is 0.4 [16]. Figure 2-13 shows the fluorescence anisotropy values for various HA solutions. LSLHA is a soil HA (Lathhco silt loam humic acid), comprising saturated hydrocarbon links; LHA contains condensed aromatic material and was associated with lignite deposits; SRHA (Ritzville soil humic acid) is an aquatic HS that possess more functional groups; SHHA has a high content of aliphatic and heteroaliphatic parts; RSHA was extracted from a sandy Ritzville soil with a relatively high aromatic content; PLVHA is an algal HA newly obtained from Pilayella littoralis and has a similar proton magnetic resonance (PMR) spectra to compost HA [16].

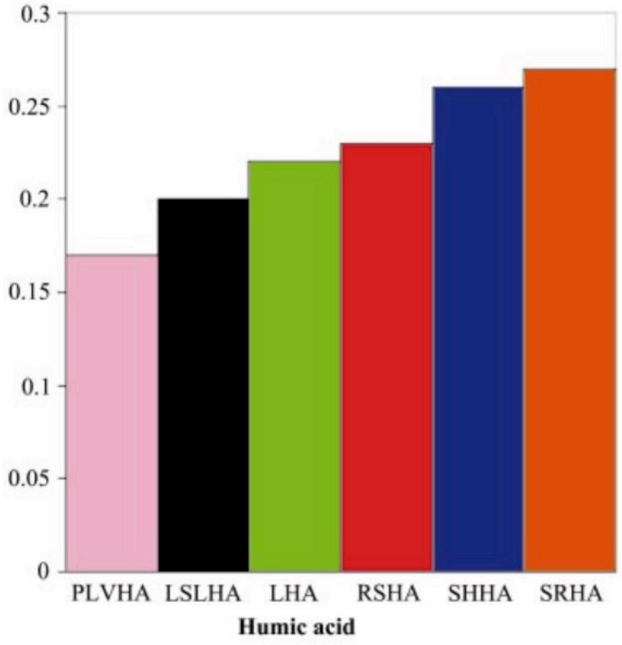

Figure 2-13 Fluorescence anisotropy values of 5 ppm HA solutions in glycerol at room temperature [16].

2.5 Objectives

This work is intended to explore the connection between humic acids and liquid crystalline domains presented in heavy oil fractions. As humic substances are potential sources of liquid crystals in bitumen, the goal of this work is to explore whether and, if so, under what conditions humic acids form liquid crystals. The formation of liquid crystal domains with homogeneous organic or aqueous cores and humic substance liquid crystalline shells dispersed in aqueous or hydrocarbon liquids in hydrocarbon-water emulsions will be addressed in this work. The factors that lead to artifact problems when using polarized light microscopy in this field are also addressed.

Chapter 3 Experimental

3.1 Materials

Humic acid (CAS-No.: 1415-93-6) purchased from Sigma-Aldrich Chemicals, comprising a range of molecular sizes with related chemical formulae, was used to prepare humic acid solutions of different concentrations. Hydrocarbons used in this work included: toluene (assay 99.9%, Fisher Scientific), hexane (assay 99.9%, Fisher Scientific), Octane (assay 99.9%, Fisher Scientific), naphthalene (Fisher Scientific), octacosane (99%, Alfa Aesar), dodecane (Fisher Scientific), and 1-Methynaphalene (97%, Acros). Their purpose was to create a water-hydrocarbon system. Anhydrous ethyl alcohol (Commercial Alcohols) was used to extract material from humic acids. Octadecyltrichlorosilane (>90%, Sigma-Aldrich) was used to process slides to obtain hydrophobic surfaces. Hellmanex III (Sgima-Aldrich) was used as a detergent for cleaning slides and test tubes.

A sample of 4′-Pentyl-4-biphenylcarbonitrile (98%, Sigma-Aldrich), which has the molecular formula $CH_3(CH_2)_4C_6H_4C_6H_4CN$, was used as a control for liquid crystalline behavior. This is a nematic liquid crystal in the temperature range 291.16 K to 298.16 K, which means that it shows liquid crystal properties at room temperature. This type of liquid crystal can assemble at oil-water interfaces, thus it is a good choice as a liquid crystal model.

3.2 Experimental Apparatus

3.2.1 Olympus GX 71 Inverted Microscope

An inverted microscope model Olympus GX 71 was used in this work (Figure 3-1). It is equipped with a polarizer and an analyzer (Olympus GX-AN 360). An image acquisition system is connected to the microscope and the images are captured and processed with Olympus Stream Software. The principles of polarized light are discussed in Chapter 2.

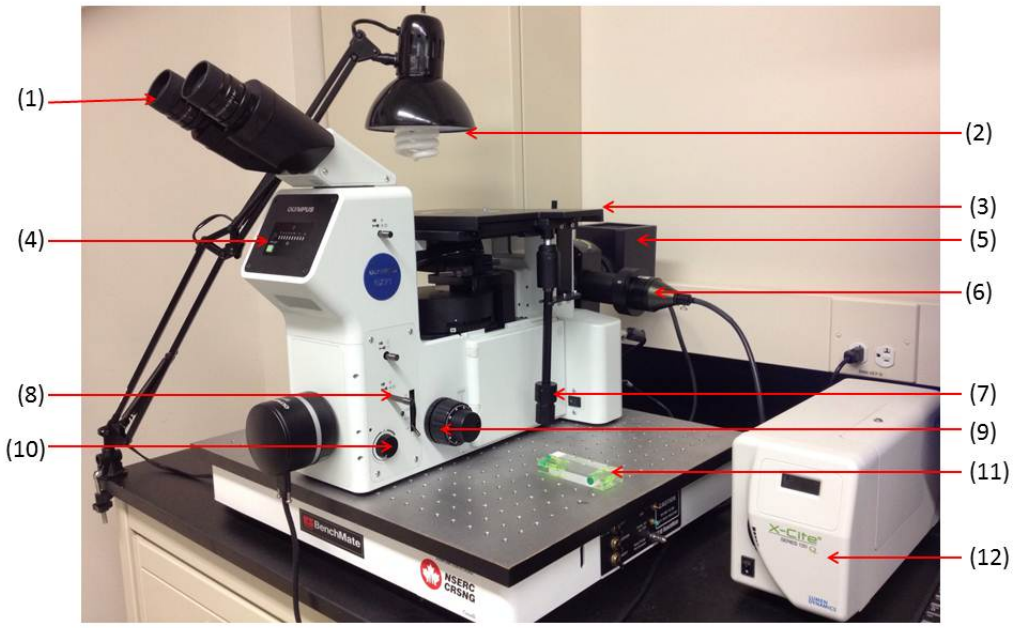

Figure 3-1 The photo of Olympus GX71 microscope in the lab: (1) Ocular lens, (2) Natural light source, (3) Mechanical stage, (4) Light intensity indicator, (5) Halogen light source, (6) Fluorescent light connector, (7) Stage drive, (8) Digital camera switcher, (9) Focus adjustment knob, (10) Light intensity controller, (11) Bubble level gauge, (12) Fluorescent light source.

3.2.2 Hot-stage microscope

A hot-stage microscope, comprised of a hot-stage reactor and an inverted reflective microscope, was used for the in-situ observation of samples during the heating. The reactor is made of stainless steel Swagelok fittings and a sapphire or yttrium aluminum garnet (YAG) window that allows samples to be observed in the microscope. The sample sits on the window and a magnetic stirrer can be used to mix the contents inside of the reactor. The microscope is equipped with crossed and parallel polarizers to detect anisotropic samples. A halogen bulb is the light source of the microscope, and adjusting the voltage can change the light intensity. A schematic diagram of the hot stage is presented in Figure 3-2.

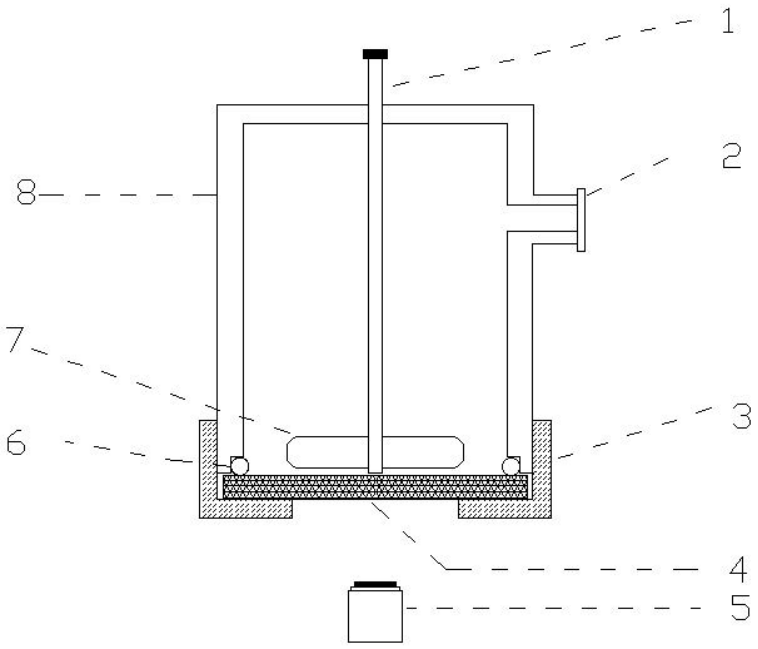

Figure 3-2 Schematic diagram of the hot-stage reactor. (1) thermocouple; (2) gas inlet; (3) bottom nut; (4) transparent YAG window; (5) objective lens of microscope; (6) O-ring; (7) magnet; (8) steel body.

3.2.3 Ultrasonic Bath

A Branson Ultrasonic Bath was purchased from Emerson Industrial Automation. This instrument was used for ultrasonic cleaning of the slides and test tubes and for the emulsification of oil-water mixtures. The temperature and time applied for the cleaning and emulsification vary according to different mixtures, and that detailed information is listed in section 3.3 and 3.8.

Figure 3-3 Ultrasonic bath.

3.2.4 Zetasizer Nano Instrument

Zetasizer Nano was used to measure the size distribution of liquid crystal spherules resulting from the self-assembly of humic acid molecules. Fine spherules are always in

constant random thermal motion, and their diffusion speeds are related to their size. At a constant temperature, the smaller the spherules are, the faster they diffuse. According to the above property, dynamic light scattering technology is embedded into the Zetasizer Nano instrument to measure particle or colloid size distributions. By illuminating the particles with a laser, a speckle pattern is produced. The scattering intensity fluctuates with time and can be detected using an avalanche photodiode detector. The curve can be then analyzed to generate the data of size distribution by a correlation function [46]. A schematic diagram is shown in Figure 3-4.

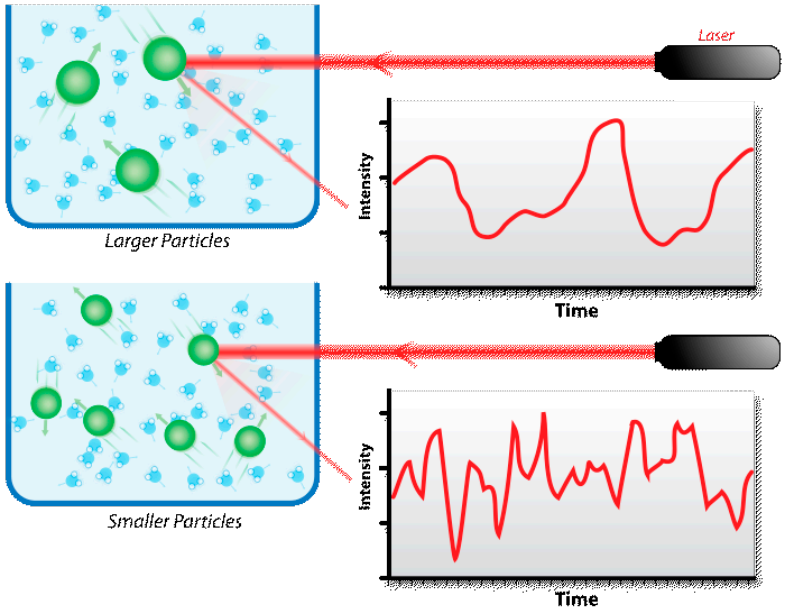

Figure 3-4 Hypothetical dynamic light scattering of two samples: Larger particles on the top and smaller particles on the bottom. [47]

Figure 3-5 Zetasizer Nano instrument for size distribution measurement.

3.3 Cleaning protocol of glass slides

The microscope slides were placed in a beaker that was filled with 200 mL deionized (DI) water; then 10 mL of Hellmanex was added. Afterward, in order to disperse the soap, the beaker was placed in an oven and heated to 353.16 K for 5 minutes. Then the beaker was placed in the ultrasonic bath for 15 minutes. Later, the microscope slides were taken out of the beaker and rinsed between 3-5 times with DI water. They were then placed in a clean beaker to be immersed in DI water and then sonicated for 15 minutes. This last procedure was repeated one more time. The cleaned microscope slides were stored immersed in DI water until needed for experiments or additional surface treatments. Clean slides should possess hydrophilic surfaces. To ensure the hydrophilic surfaces, it is vital to test the surfaces of the slides to see if water beads up. If it does, there won't be good contact between the microscope slides and the sample. Microscope slides must be rewashed until a hydrophilic surface is achieved.

3.4 Thermotropic phase change of humic acids

Thermotropic liquid crystals show phase change if heated. To check that whether solid humic acids could transform into a liquid crystalline phase when they are heated, humic acid powders were observed by hot stage microscopy during heat treatment. A mass of 7 mg of ground humic acid powders were placed on a YAG window and inserted at the bottom of an atmosphere and temperature-controlled reactor (Figure 3-2). The powders were heated at a heating rate of 5-10 K per minute under an atmosphere of nitrogen, pressurized at 1 atm. The sample was heated from room temperature, 296.16 K, to 600.76 K and one image was captured every 60 s, at a combined magnification of 100× under cross-polarized light. The temperature range of heat treatment was determined by results obtained from differential scanning calorimetry (DSC) analysis. As humic acids showed endothermic peaks on differential scanning calorimetry profiles at 370.16 K and 570.17 K, these two temperatures were chosen as endpoints to examine the potential emergence of phase change. The differential scanning calorimetry data is shown in Appendix I.

3.5 Liquid crystalline properties of the anhydrous ethyl alcohol extracted humic acids

Humic acids are partially dissolved in anhydrous ethyl alcohol. The optical properties of the extracted humic acids (EHA) were detected under an inverted microscope using polarized light. In the extraction experiments, The humic acid powders were mixed with anhydrous ethyl alcohol at mass ratios of 19.7:1 (sample 1) and 19.7:2 (sample 2), respectively. The mixtures were shaken for 5 minutes using a GVM-AS Variable Speed

Vortex Mixer and then rested for 12 hours. Afterward, the upper transparent layer was removed and transferred to a clean container for further use. Slides with hydrophilic and hydrophobic surfaces were used in this observation. Figure 3-3 shows the mixture of humic acid plus anhydrous ethyl alcohol (left) and the extracted humic acid (right). The surfaces of the cleaned microscope slides are hydrophilic (following the cleaning protocol listed in section 3.3). The surfaces of cleaned slides were turned into hydrophobic after processing with octadecyltrichlorosilane (OTS). The protocol followed is listed below.

0.2 mL of OTS is added into 100 mL of toluene by using a pipette to reach an concentration of 0.2%; Cleaned slides were immersed into the OTS solution and incubated for 15 – 20 minutes. Afterward, the slides were transferred to a beaker containing pure toluene to remove the excess OTS. The microscope slides surfaces were then dried with a pressure air gun, and placed in the oven at 363.16 K for at least 30 minutes. In the final step, the microscope slides are taken from the oven; once cooled down, they are immersed in toluene and placed in the ultrasonic bath for 5 minutes.

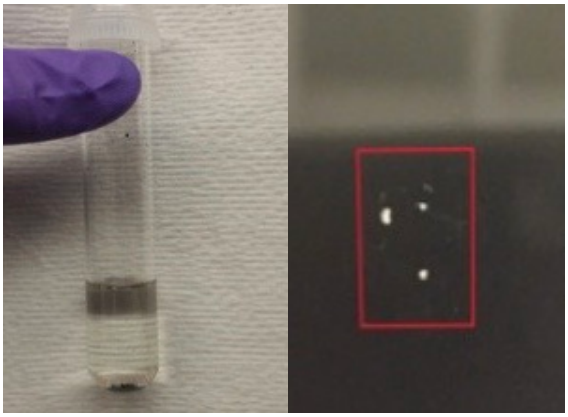

Figure 3-6 Left: a mixture of humic acid + anhydrous ethyl alcohol; right: extracted humic acid on a slide.

3.6 Liquid crystals in mixtures of humic acids and water

3.6.1 Effect of different concentrations

This experiment aims to verify that humic acids can form lyotropic liquid crystals when dispersed in water. The critical micelle concentration of humic acids in water is around 7 g/L [44]. Humic acid solutions of different concentrations were prepared and filtered (Whatman, Grade 1 paper filter) to remove insoluble materials. As the amount of insoluble materials present in the humic acid solutions was slight, their effect on the concentration was neglected. The concentrations used were 2 g/L, 8 g/L, and 12 g/L. In order to check the formation of anisotropic droplets, samples were placed on the microscope slides using pipets and observed under polarized light.

3.6.2 Effect of temperature on the liquid crystal droplets formation

The concentration of humic acid solution used in this experiment was 8 g/L. This concentration meets the requirement of the Zetasizer Nano unit. Four vials filled with 5 mL of the filtered humic acid solution were prepared. The filter paper used here is Grade 1 and provided by Whatman. One of the vials was kept at room temperature (293.15 K), and the other three were heated to 333.15 K, 353.15 K, and 363.15 K respectively for 30 minutes. Particle size values for each sample were collected.

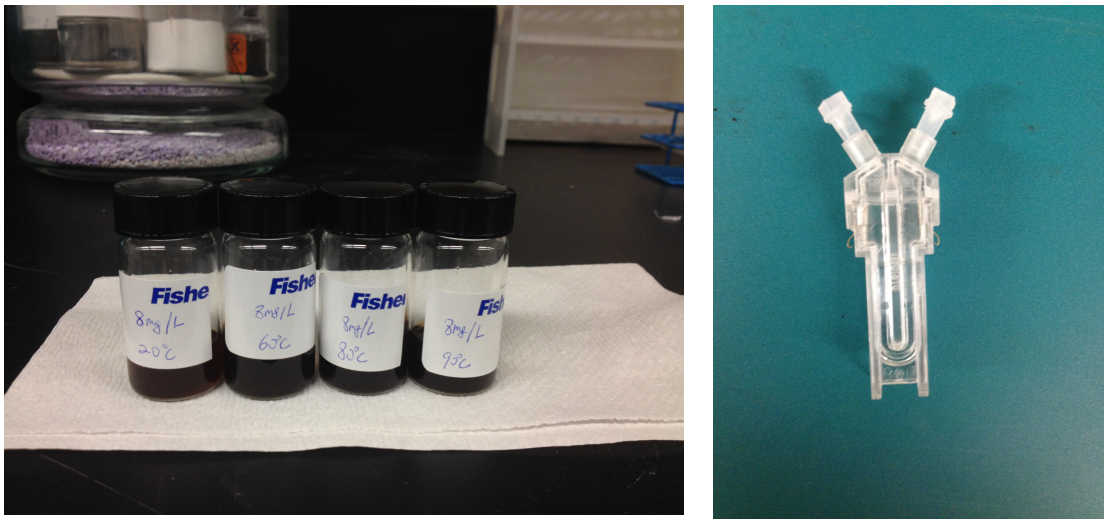

Figure 3-7 Left: Vials filled with a filtered humic acid solution; right: dip cell used in Zetasizer Nano instrument.

3.7 Artifacts

3.7.1 Light interference among droplets

Droplets in water usually lead to light scattering, inter-refraction, and inter-reflection among each other. The light interference among droplets may affect the brightness of droplets under polarized light [48]. Two control samples were prepared by adding 10 drops of hexane in 60 mL of water (sample 3), and 30 drops of hexane in 60 mL of water (sample 4). Both samples were emulsified for 1 minute using an ultrasonic bath and then they were observed under the microscope under polarized light and normal light. During the observation, the light source intensities of the microscope applied to both samples were kept the same.

Table 3-1 Composition of mixtures of sample 1-2

Sample	D.I water/mL	Hexane/drops
3	60.0	10
4	60.0	30

3.7.2 Differences of refractive index

The difference in refractive index between hydrocarbon liquid and water may also affect the appearance of artifacts [31,49]. For the light of the same wavelength, different oils possess different refractive indexes. Table 3-2 shows some examples. In this experiment, three different hydrocarbons were dispersed in water. 3 mL of DI water, a drop of octane, toluene, and 1-methylnaphathlene were added to each vial, respectively. Afterward, the three mixtures were emulsified in the ultrasonic bath for 1 minute. The octane-water mixture was then diluted by adding 3 mL of water; the toluene-water mixture and the 1-methylnaphathlene-water mixture were diluted by adding 6 mL and 18 mL of water respectively. Different species of hydrocarbons can disperse different numbers of droplets into the water after a specific time of emulsification. This dilution process made it possible to keep the same number of hydrocarbon droplets appearing in the view of observation to eliminate the interferences between multiple oil droplets that were illustrated in section 3.7.1. The diluted samples were observed by the microscope under polarized light. The images were taken at a light intensity of 12 (microscope light intensity range 0-12).

Table 3-2 Refractive indices of fluids [49]

Medium	Refractive index	Light wavelength/nm
Water	1.3314	640.7
Octane	1.3973	640.7
Toluene	1.4931	640.7
1-Methylnaphathlene	1.6160	640.7

3.7.3 Curvature of droplet interface

Water droplets spread on slides with different surface properties exhibit different contact angles, and the curvatures of the droplet surfaces are different. Two types of slides were utilized in this experiment. The first one corresponds to the OTS processed slides, which possess a hydrophobic surface that can lead to contact angle around 90 degrees. The other type of microscope slides used were purchased from Fisher Scientific (Fisherfinest™, ER#5X501FF), processed only with the necessary cleaning steps using DI water and soap. These slides did not follow the cleaning protocol presented in section 3.3 to avoid impairing the hydrophobic surfaces. The contact angles of water droplets on this slide were much lower than 90 degrees. Micro DI water droplets were spread on surfaces of slides using a Hamilton syringe and observed under the microscope. The brightness of the pattern of water droplets faded under polarized light as the droplet surface curvature decreased. This fading process was recorded.

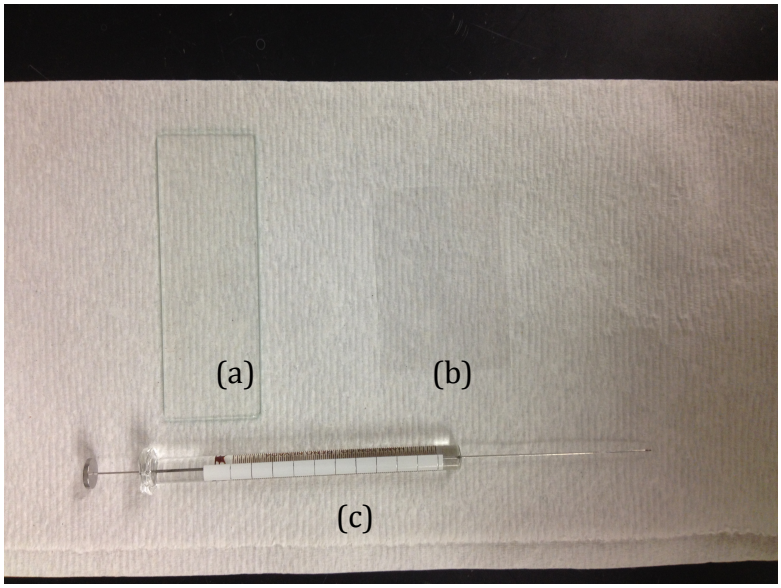

Figure 3-8 (a) OTS processed slide; (b) None-processed slide; (c) Hamilton syringe.

3.8 Formation of liquid crystal layer by humic acid at water/hydrocarbon and water/water interfaces

It has been reported that a separate phase on the exterior surfaces of hydrocarbon drops can be formed, showing liquid crystalline properties, which is described as a biplex structure [1]. Liquid crystal layers that coat oil drops increase the rigidity of the interface and prevent fingering and, thus enhance the stability of an emulsion or foam [7, 8]. Therefore, the formation of liquid crystal domains with homogeneous organic or aqueous cores and humic acid liquid crystalline shells dispersed in aqueous or hydrocarbon liquids in hydrocarbon-water emulsions is worth exploring. This role that humic acids play in water-hydrocarbon mixtures may affect the efficiency of the water de-oiling process in

the oil industry and affect the treatments needed to remove hydrocarbon content from recycled water. In this part, experiments were designed with the aim to create biplex droplets in mixtures of water + hydrocarbon.

3.8.1 Hydrocarbon-external-water structure

Liquid hydrocarbon droplets dispersed in water show a Maltese cross pattern if they are observed under polarized light. Figure 2-2 presents an example of toluene droplets dispersed in water. In this case, it cannot be distinguished easily whether humic acids form a liquid crystal layer at the interface of water and hydrocarbon. However, liquid hydrocarbon droplets do not retain a biplex structure when the surrounding water dries out. Therefore, octacosane, with a melting point at 334.46 K, was used to create hydrocarbon droplets in water bulk. Little octacosane is lost during the drying process.

Four samples, 5, 6, 7, and 8, were prepared. Mixtures were put in four test tubes separately and were processed in four steps. The compositions of samples in the test tubes are listed in Table 3-3. A beaker filled with water was used as the heating bath (see Figure 3-9). The test tubes were immersed in the heating bath and heated to 335.16 K; the samples in the test tubes were emulsified by ultrasonic bath for 3 minutes. This process was repeated five times to make 20 mL of each sample. The samples were transferred to centrifugation tubes, and they were centrifuged for 45 minutes at 18,000 rpm at 301.16 K. At last, four samples were prepared, and their composition is listed in Table 3-4.

Table 3-3 Compositions of mixtures for sample making

Test tube	D.I water/mL	Humic acids/mg	Octacosane/mg	4′-Pentyl-4-biphenylcarbonitrile/μL
A	4.0	20.0	2.0	0
B	4.0	0	2.0	0
C	4.0	20.0	0	0
D	4.0	0	2.0	0.2

Table 3-4 Compositions of mixtures of sample 5-8 for centrifugation

Sample	D.I water/mL	Humic acids/mg	Octacosane /mg	4′-Pentyl-4-biphenylcarbonitrile/μL
5	73.9	100	10	0
6	74.1	0	10	0
7	74.0	100	0	0
8	74.0	0	10	1

One drop of each sample was pipetted from the dense sample area and placed on different glass slides; then, they were observed under the inverted microscope under (polarized / normal light) where images were captured. After the observation, the microscope slides were put back in the vacuum oven, and they were heated to the temperature corresponding to the melting point of octacosane i.e., 334.46 K. The heating was halted once the octacosane particles seem melted (naked eye observation). This process took around 60 seconds if the oven is preheated to 333.16 K. Once the microscope slides temperature dropped to room temperature (295.16 K), they were observed under the

microscope again.

Sample D was prepared as control by using a type of nematic liquid crystal purchased from Aldrich Scientific, 4′-Pentyl-4-biphenylcarbonitrile (5CB). This sample was used to compare with the result of samples 5, 6, and 7.

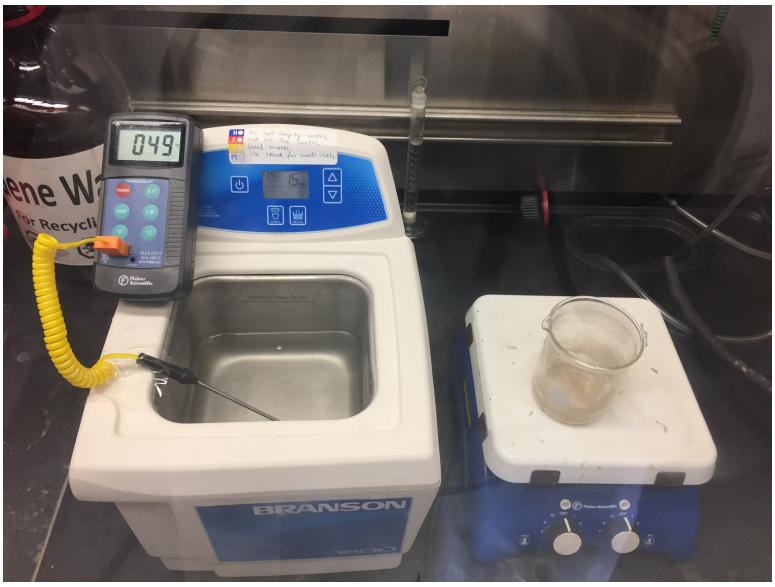

Figure 3-9 Photo of heating bath and ultrasonic bath.

3.8.2 Water-external-water structure

As discussed in Chapter 2, there are four possible forms of biplex structures in hydrocarbon-humic acids-water mixtures. This experiment's main goal is to explore whether humic acids form a liquid crystal layer at the interface of the bulk water and a hydrous core. Five samples, 9 – 13, were prepared following the steps below. Water in the heating bath and the ultrasonic bath was controlled in the temperature range of

366.16-368.16 K and 323.16-328.16 K, respectively. Test tubes containing mixtures were immersed in the heating bath to melt the solid hydrocarbon for 50 seconds. Afterward, the test tubes were transferred to the ultrasonic bath and kept there for 30 seconds. Sample 11 is prepared by emulsifying a 4′-Pentyl-4-biphenylcarbonitrile and water mixture to work as a control. The compositions of the five samples are listed in Table 3-5.

Table 3-5 Compositions of mixtures of sample 7-11

Test tube	D.I water/mL	Humic acid (HA)/mg	Naphthalene/ mg	4′-Pentyl-4-biphenylcarbonitrile/μL	Concentration of HA in water/g/L
9	4	4.8	1.5	0	12
10	4	0	1.5	0	0
11	4	4.8	0	0	12
12	4	24	1.5	0	60
13	4	0	0	1	0

Because naphthalene emits vapor when heated, it is recommended to perform all the experiments in a fume hood. During the naphthalene melting process, attention should be taken to avoid over-heating; otherwise, some naphthalene evaporates. In this experiment, temperature control is critical to the formation of the biplex structure with a hydrous core and surrounded by water.

3.8.3 Water-external-hydrocarbon structure

To explore whether humic acids form a liquid crystal layer at the interface of water droplets in hydrocarbons, mixtures of dodecane, humic acid, and water were prepared and observed. Two samples, 14 and 15, were prepared in test tubes. The compositions of these samples are listed in Table 3-6. Both samples were emulsified in an ultrasonic bath for 5 minutes and then drops were pipetted onto slides to be observed under the microscope. Light intensity was kept the same when observing the two samples under polarized light.

Table 3-6 Compositions of mixtures of sample 12 and 13

Sample	D.I water/mL	Humic acid/mg	Dodecane/mL	HA Concentration in water/g/L
14	0.1	0.005	3	50
15	0.1	0	3	0

To demonstrate that the liquid inside of the liquid crystal interface layer is water, a water-based coloring agent was used to color the water (Figure 3-10). 0.1 mL of this coloring agent was diluted into 5 mL of D.I water to color it green. The experiments in section 3.8.3 were repeated and samples were observed under the microscope to confirm whether the green color appears inside or outside of the droplet. If the color green is observed in the inner domain, it means that a water-external-hydrocarbon structure is created.

Figure 3-10 Photo of water-based coloring agent**.**

Chapter 4 Results and Discussion

4.1 Thermotropic phase change of humic acids

The optical properties of humic acid were examined from room temperature, 296.16 K, to 600.76 K. Liquid crystal formation was not observed with increasing temperature in this range. Figure 4-1 shows images of humic acid under polarized light at different temperatures. Solid humic acids caused the relatively bright areas. These solids did not show liquid crystalline characteristics nor the process of melting on increasing temperature. As humic acids did not show phase change during heating, it suggests that humic acids on their own do not form thermotropic liquid crystals in this temperature range. DSC was performed on humic acid solids. Two endothermic peaks showed at 370.16 K and 545.17 K (see Appendix I). The endothermic peaks can be attributed to dehydration and to the decomposition of large molecules of humic acids instead of the thermotropic phase change. This result is consistent with thermogravimetric analysis of humic acid that demonstrated decomposition [50].

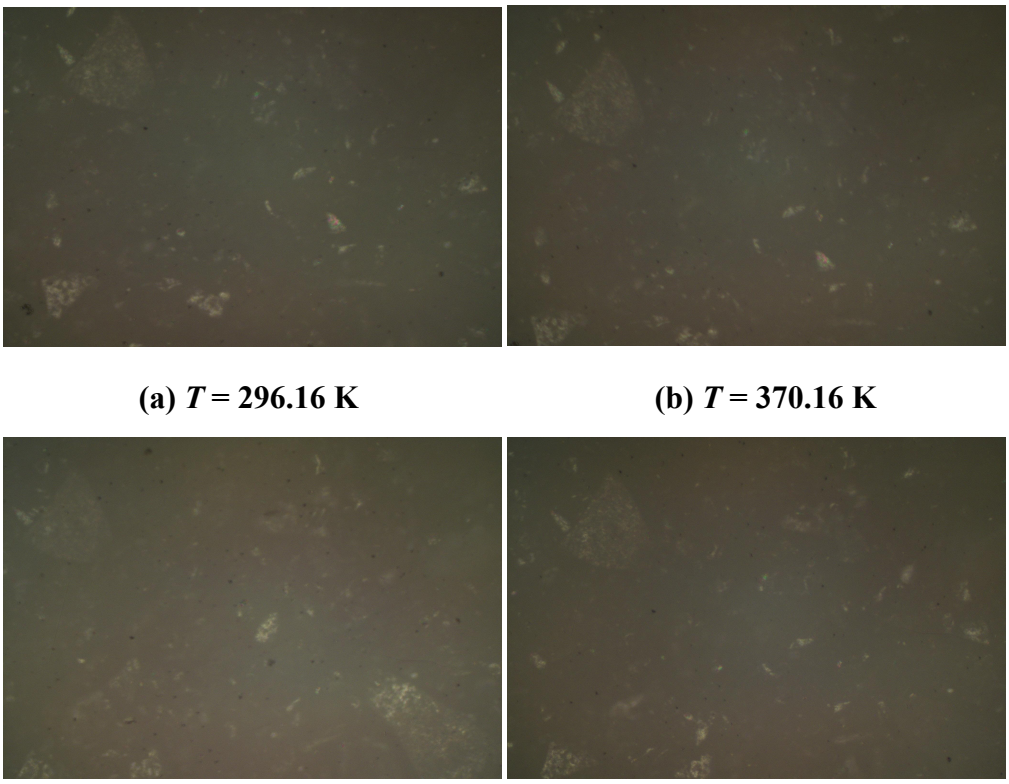

(a) T = 296.16 K **(b) T = 370.16 K**

(c) T = 545.17 K **(d) T = 600.76 K**

Figure 4-1 Humic acids powders under polarized light at 100x magnification.

4.2 Liquid crystalline properties of the anhydrous ethyl alcohol extracted humic acid

According to Figure 4-2, the ethanol extracted humic acid (EHA) shows liquid crystalline properties when sitting on OTS processed hydrophobic slides as Maltese cross shape can be clearly observed under cross-polarized light. Image *a* and *b* are of sample 1 with a mass ratio of 19.7:1 (ethanol to humic acids) and image *c* and *d* are of sample 2 with a mass ratio of 19.7:2 (ethanol to humic acids). Image *a* and *c* were taken under cross-

polarized light and image *b* and *d* were taken normal regular light. Both samples of the two different mixture ratios show the existence of liquid crystals, and the texture shape under cross polarized light is that of a Maltese cross. Under normal light, the spherules of liquid crystals can be clearly observed. For sample 1, the size of the liquid crystals is around 2 to 4 μm; for sample 2, the size of the liquid crystals can be as large as 5 μm. Liquid crystal spherules extracted from samples with a higher humic acids-to-ethanol mass ratio present a larger size than that from samples with a lower ratio, but the difference is not significant. The pattern of the liquid crystals on OTS processed hydrophobic slides does not change when the extraction conditions change. Figure 4-3 shows the results observed after sample 2 on slides was incubated for 120 days at ambient conditions in the laboratory. Images in Figure 4-3 were captured at different analyzer-to-polarizer angles to verify the anisotropic properties of EHA [51]. Definite birefringence occurs at 0º, showing Maltese cross patterns, and the patterns change along with the change of the analyzer-to-polarizer angle. Images taken at 45º and 90º show colorful stripes and irregular shapes, which correspond with properties of liquid crystals [52]. The size of the liquid crystal droplets after the incubation is much larger than that shown in Figure 4-1, and they can reach 10 to 20 μm. Small liquid crystalline droplets merge into larger droplets during the incubation period while keeping the liquid crystalline property unchanged. These samples are sealed and don't sorb moisture from the laboratory air.

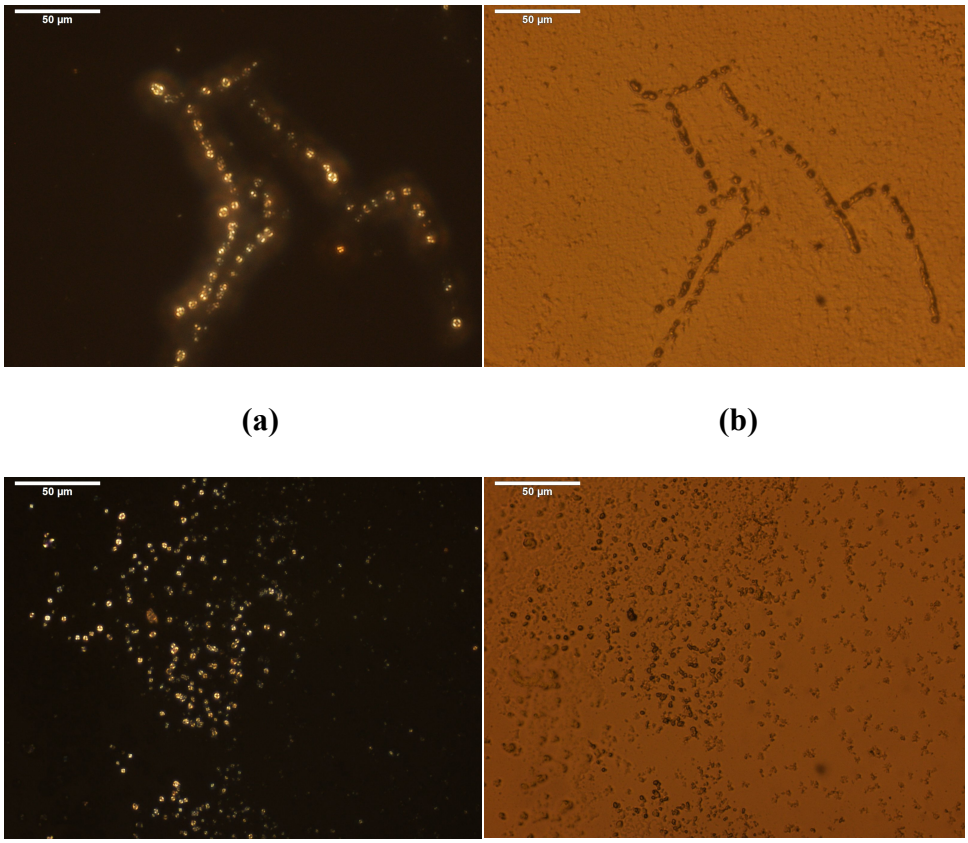

Figure 4-2 EHA on OTS processed hydrophobic slide: (a) under polarized light of sample 1; (b) under normal light of sample 1; (c) under polarized light of sample 2; (d) under normal light of sample 2.

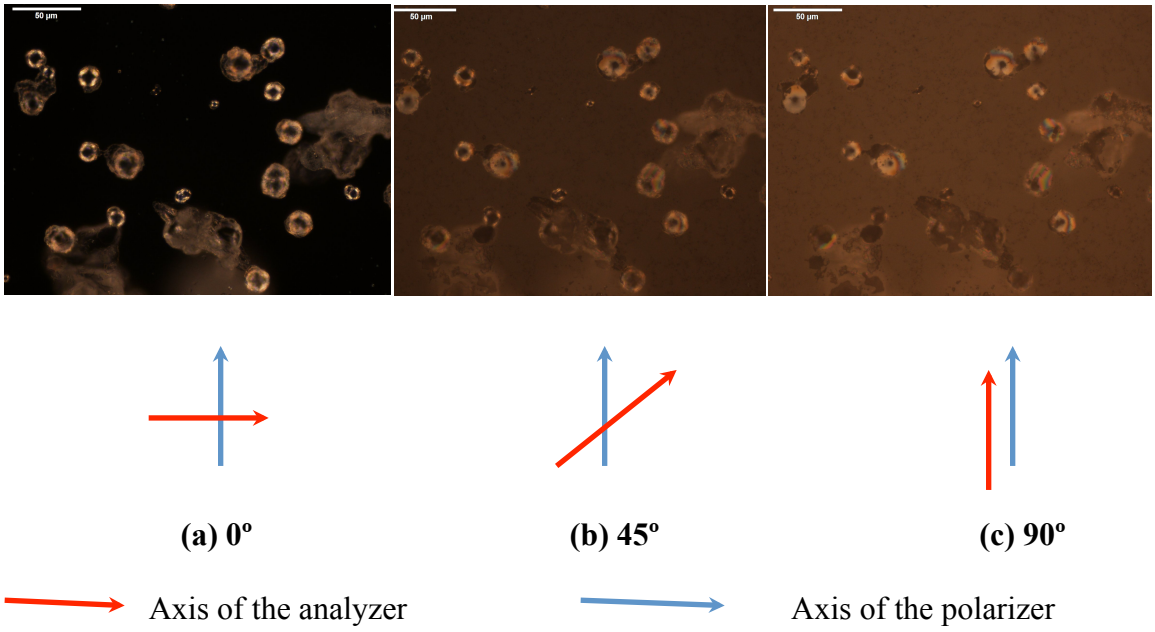

Figure 4-3 Incubated EHA on OTS processed hydrophobic slide: (a) analyzer at 0º; (b) analyzer at 45º; (c) analyzer at 90º.

The EHA sitting on hydrophilic slides was also observed, and Figure 4-4 presents the results. Both samples show anisotropic properties under polarized light. Fan-shaped textures arise under polarized light in sample 1 (see image *a* in Figure 4-4), which is one of the typical textures that liquid crystals can present [27, 53, 54, 55]. The patterns of sample 1 (see image *b* in Figure 4-4) under normal light appear as irregular plates that differ from those angular patterns of solid crystals. Textures observed in sample 2 (see image *c* in Figure 4-4) look different, and they are highly condensed. The textures present high birefringent properties under polarized light and the fan-shaped patterns are apparent even if the textures overlap with one another. This result reflects that the increased concentration of EHA in anhydrous ethyl alcohol could increase the volume of a single liquid crystal droplet and therefore led to more condensed patterns. The image of sample

2 under normal light (see image *d* in Figure 4-4) presents liquid-like droplets. The droplets contact each other and the thickness appears larger than that of sample 1. The crowded droplets help explain why the fan-shaped patterns under polarized light connect with each other and appear on top of one another.

The liquid crystalline textures presented by EHA on the hydrophilic slides are nematic [53,56]. Hu and Jang [27] explained similar features of liquid crystals using 5CB, which is a well-known liquid crystalline material. Solutions of 5CB in ethyl alcohol were placed on hydrophilic slides and OTS-treated hydrophobic slides, respectively, and were observed under polarized light. A flower-like texture was observed, instead of a fan-shaped texture, in the case of a higher 5CB concentration in an ethyl alcohol solution. Three patterns that 5CB presents under polarized light are shown in Figure 4-5. Comparing to the results of Hu and Jang [27], the optical properties of EHA agree well with that of 5CB. Both 5CB and EHA present texture change on hydrophilic slides when their concentration in ethyl alcohol is altered, and both of the two species show Maltese cross pattern on OTS processed hydrophobic slides.

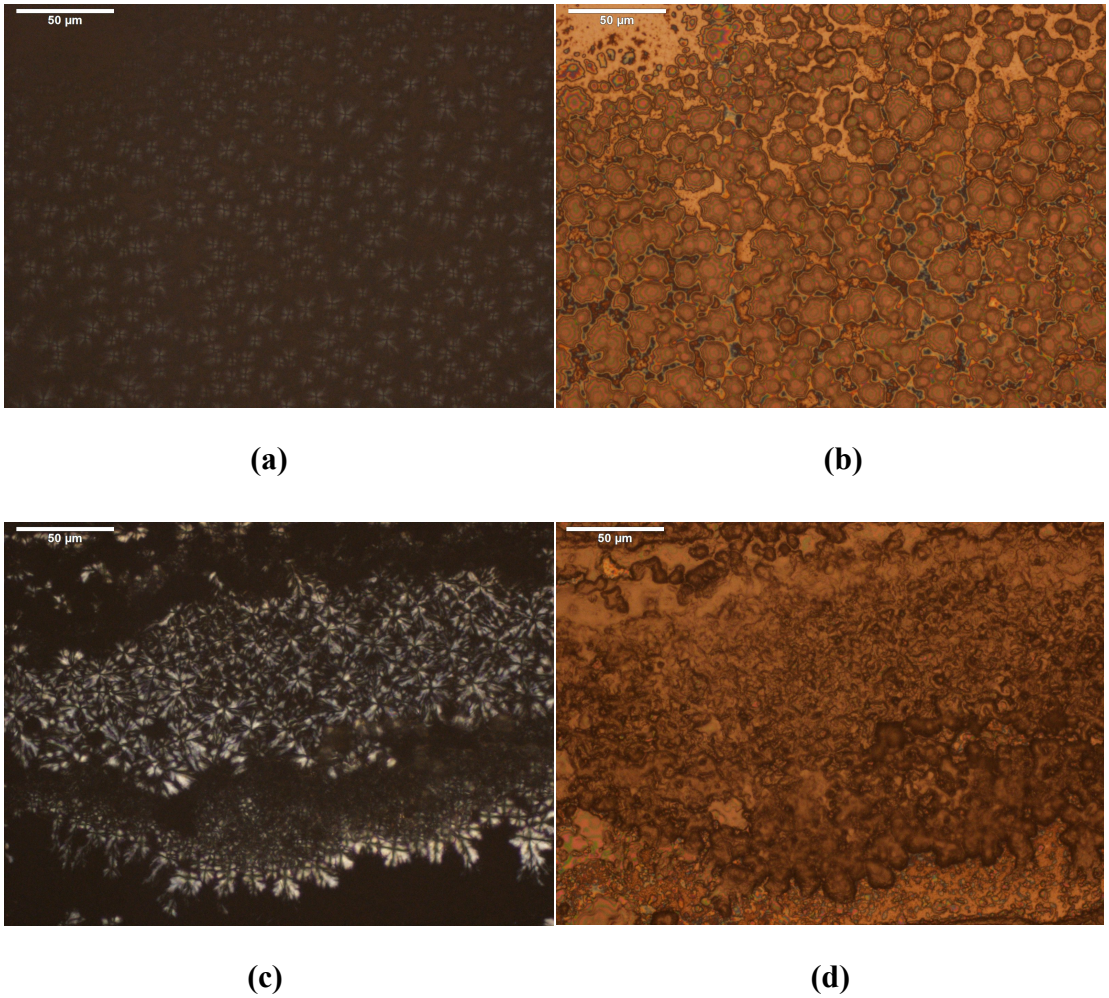

Figure 4-4 EHA sitting on hydrophilic slide: (a) under polarized light of sample 1; (b) under normal light of sample 1; (c) under polarized light of sample 2; (d) under normal light of sample 2.

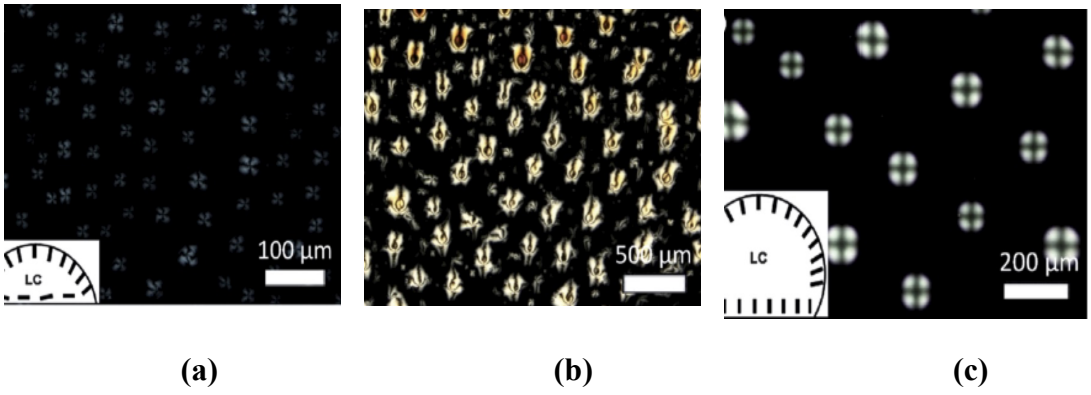

Figure 4-5 Different patterns of 5CB under polarized light: (a) fan-shaped pattern; (b) flower-like pattern; (c) Maltese cross pattern. [27]

In summary, ethanol extracted humic acid (EHA) possesses a liquid crystalline phase. Its behavior parallels that of a control material (5CB) in three ways:

- it possesses textures showing anisotropic properties under cross-polarized light similar to those of 5CB.
- these patterns change like those of 5CB when hydrophobic slides are replaced by hydrophilic slides.
- textures change when the concentration of EHA in anhydrous ethyl alcohol is altered analogously to 5CB.

4.3 Liquid crystals in mixtures of humic acid and water

4.3.1 Effect of concentration

Humic acid solutions of three concentrations were observed under polarized light, respectively. Figure 4-6 presents the results. For the solution of concentration 2g/L, no optic patterns were observed. For solutions of concentration 8g/L and 12g/L, Maltese cross patterns were observed, which demonstrate the anisotropy of humic acid spherules. Humic acids are large amphiphilic molecules. Their self-assembly leads to the formation of anisotropic spherules in water bulk [57]. Considering the definition of lyotropic liquid crystals [58] and the fact that the CMC of humic acids is around 7g/L, it is sound to deduce that humic acid molecules can form lyotropic liquid crystalline spherules in water solution. The essence of these lyotropic liquid crystalline spherules is supermolecular structures that show anisotropic optic properties. The sizes of the liquid crystalline

droplets do not change significantly after the concentration surpasses the CMC (see image *b* and image *c* of Figure 4-6). This result agrees well with the work of Guetzloff and Rice [44]. They studied micelles formed by humic acids in aqueous environments and found that the micelle size did not show an abrupt change as the concentration increased from below to above the CMC value. Researchers also reported some other cases of liquid crystals formation using surfactants, such as PEG-8 Distearate (CAS NO. 9005-08-7), non-Chiral N-Acylamino acid, and sodium naphthenates [59-61]. The findings in this work parallel the results of these other researchers: humic acid, as a kind of surfactant composed of amphiphilic molecules, can also form liquid crystals with water participated.

(a)

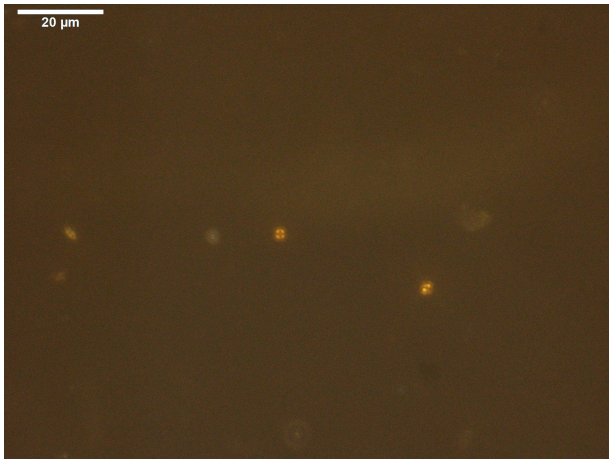

(b)

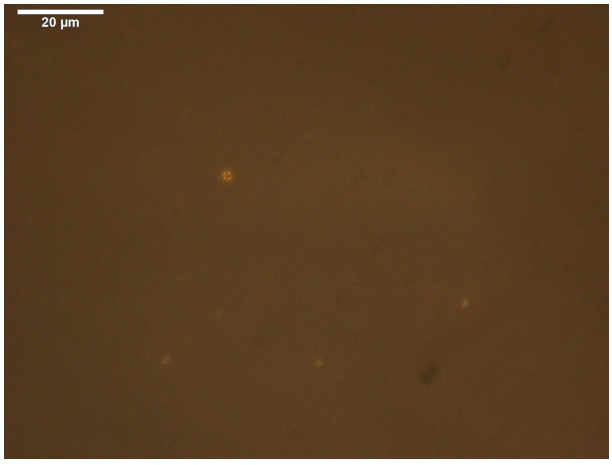

(c)

Figure 4-6 Humic acid in water at: (a) 2g/L; (b) 8g/L; (c) 12g/L.

The liquid crystalline droplets stayed on the slide even after the bulk water evaporated. Figure 4-7 shows the liquid crystalline droplets observed on hydrophobic slides after the water of humic acid solution evaporated. The Maltese cross pattern can be clearly observed in image *a*. The red arrows indicate the corresponding places of the liquid crystalline droplets in the two images. The original concentration of this humic acid solution was 5g/L, below the CMC value. However, with the evaporation of water, the concentration exceeds the CMC, which explains the formation of liquid crystalline textures. Figure 4-8 presents a fan-shaped pattern of liquid crystals formed by humic acids on hydrophilic slides. This behavior was discriminated from the behavior of isotropic drops in water. Solution concentrations used in both of the two observations were kept low because a higher concentration would introduce more interferences such as minerals in humic acids. These materials could interrupt the observation of liquid crystals. The slides carrying the liquid crystal droplets were kept in room environment for 24 hours, and it turned out that the Maltese cross pattern disappeared, with only patches of birefringent solids remaining, which means the liquid crystals are unstable unless they are in a water-saturated environment.

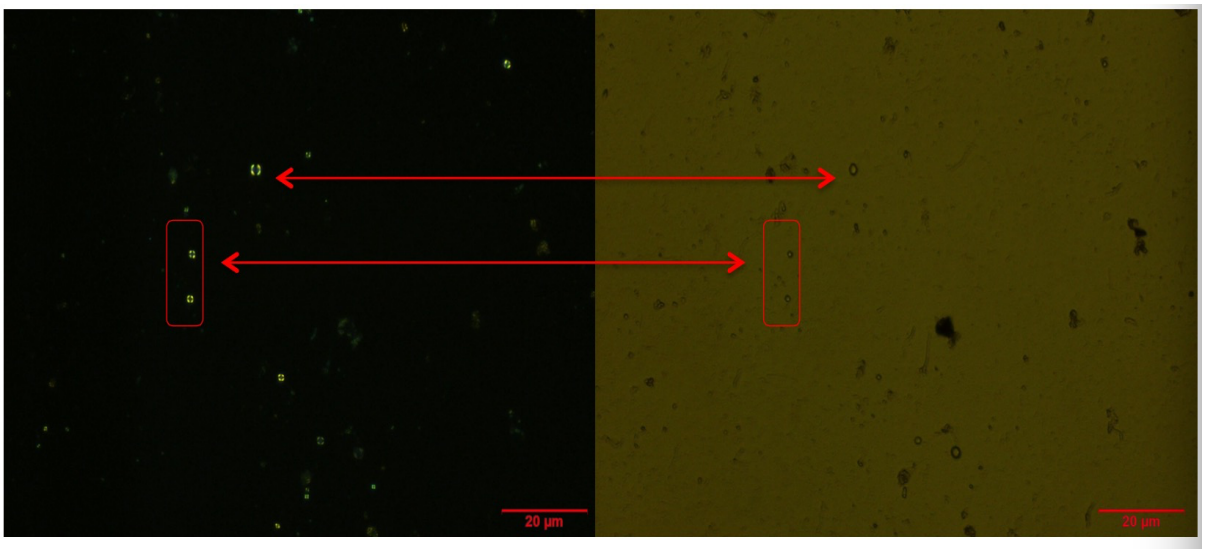

(a) **(b)**

Figure 4-7 Humic acids in water with an original concentration of 5g/L (water evaporated): (a) under polarized light; (b) under normal light.

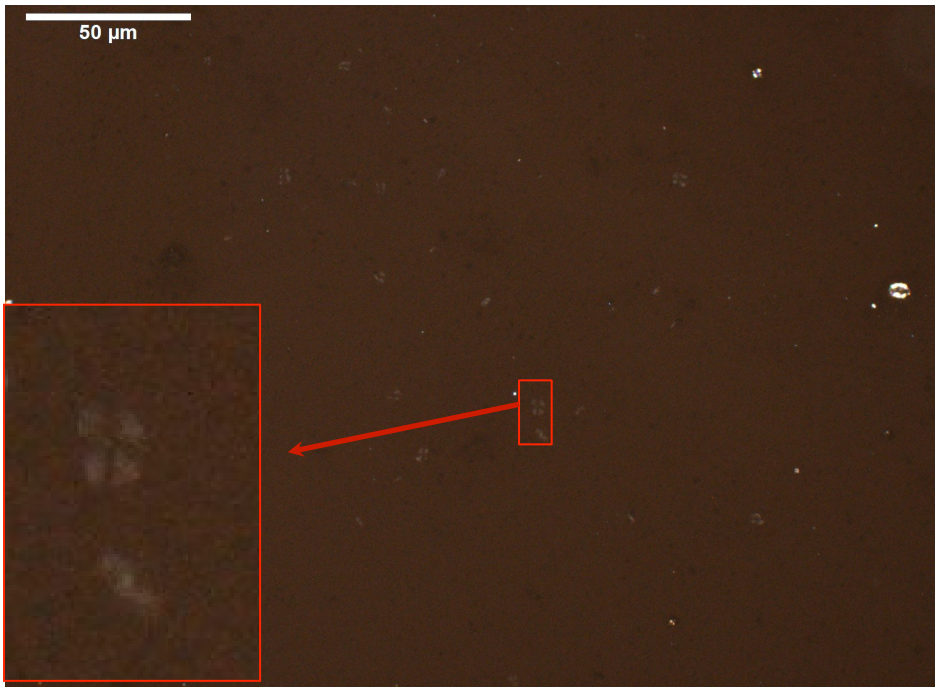

Figure 4-8 Humic acids in water with an original concentration of 2g/L (water evaporated) under polarized light.

4.3.2 Effect of heating on liquid crystal spherules formation

The self-assembly of amphiphilic molecules is usually temperature-dependent [62]. As the experiment concerning of octacosane-HAs-Water system in section 4.5 was going to be implemented above the melting point of octacosane, figuring out how the liquid crystal formation performs along with the temperature is necessary. Humic acid solution with a concentration of 8 g/L was filtered by a Whatman Grade 1 filter paper to remove the insoluble materials before being heated at different temperatures.

Particle size distributions are expressed as number or volume distributions. The distribution data express the fraction or percentage that size classes possess in a total distribution. Distributions by volume, emphasize the influence of larger objects. Size distributions by number, typically give greater emphasis to smaller drops [63]. As the liquid crystalline spherules cover a broad size range, from 20 – 600 nm, the data are presented on a number basis. Figure 4-9 shows that the number peaks of the size distributions shift to larger values (from ~ 30 nm to ~ 90 nm as the temperature is increased from 293.15 K to 363.15 K) and that the distributions broaden as temperature increases. These values and ranges are much smaller than the 2 – 4 μm sizes observed by polarized light microscopy, which emphasizes the very largest and hence rare objects in these distributions.

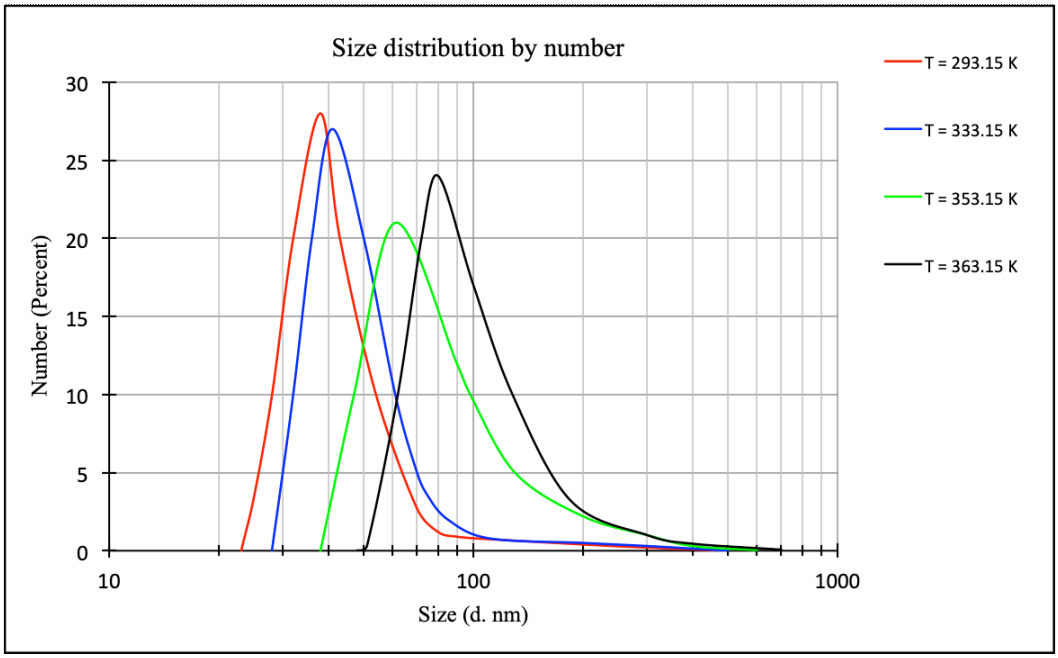

Figure 4-9 Size distribution of liquid crystalline spherules in HAs-water solution; heated under different temperatures

4.3.3 Summary

Humic acid shows lyotropic liquid crystalline properties with the participation of water. Heating the water-humic acid solution promotes the formation of larger liquid crystalline spherules. The results of this experiment provide prerequisite support for the experiments in Section 3.8, which explore the formation of biplex structure in water-HA-hydrocarbon mixtures. For this latter work, the formation and stability of hydrocarbon-external-water liquid crystalline domains over the temperature range 293.15 K to 335.15 K are critical.

4.4 Artifacts

4.4.1 Light interference among droplets

Figure 4-10 comprises images captured of sample 3 and sample 4 (see Table 3-1) by a polarized microscope. The amount of hexane added to sample 4 is three times of that of sample 3. Under normal light, more hexane droplets of sample 4 (image *d* in Figure 4-9) can be observed in the scope than that of sample 3 (image *b* in Figure 4-9). Under polarized light, hexane droplets of sample 4 (image *c* in Figure 4-9) show Maltese crosses, yet there is no Maltese cross observed in the scope of sample 3 (image *a* in Figure 4-9). If more droplets appear in a specific volume of water, the level of light scattering, inter-refraction and inter-reflection will be higher. By comparing the results of sample 3 and sample 4, light interference among droplets in water bulk is an artifact that leads to the appearance of a Maltese cross pattern.

The consequence of this artifact increases the difficulty of identifing the appearance of liquid crystals when exploring the hydrocarbon-external-water structure in the oil-HAs-water system. Therefore, octacosane was used in section 4.5 to avoid the interruption of artifacts as octacosane is in the solid phase at room temperature.

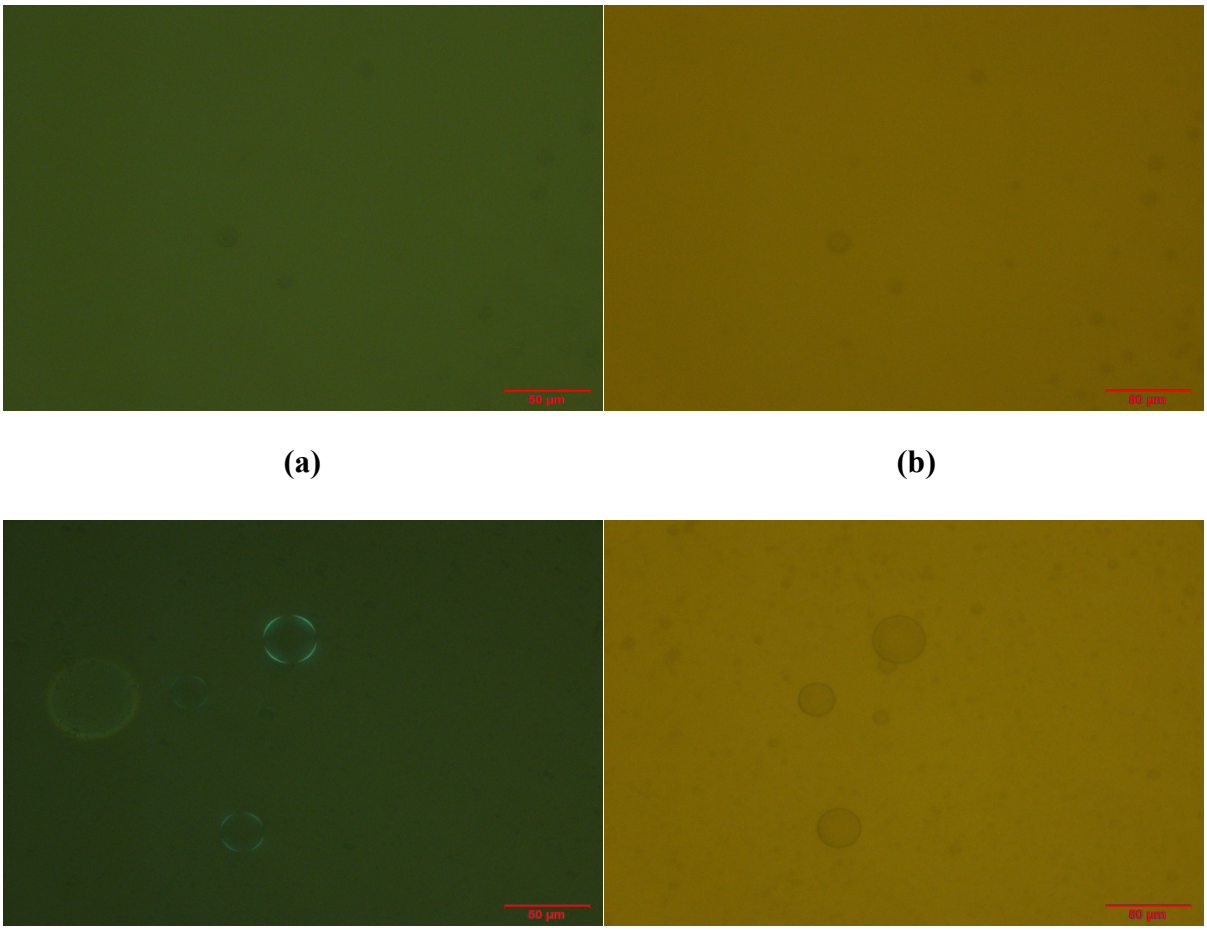

(a) **(b)**

(c) **(d)**

Figure 4-10 Hexane droplets in water: (a) under polarized light -sample 3; (b) under normal light -sample 3; (c) under polarized light-sample 4; (d) under normal light - sample 4.

4.4.2 Differences of refractive index

Figure 4-11 shows that the droplets of octane, toluene, and 1-Methylnaphathlene present Maltese cross pattern, under polarized light, respectively, but the brightness of the patterns is different. The hydrocarbon that possesses a higher difference of refractive index from water presents a brighter pattern. The amount of droplets in the view of observation is roughly the same, which helps avoid the interference difference of light

refraction between hydrocarbon droplets. It is evident that the value of the refractive index is an artifact that can introduce the appearance of Maltese cross pattern in the oil-in-water system.

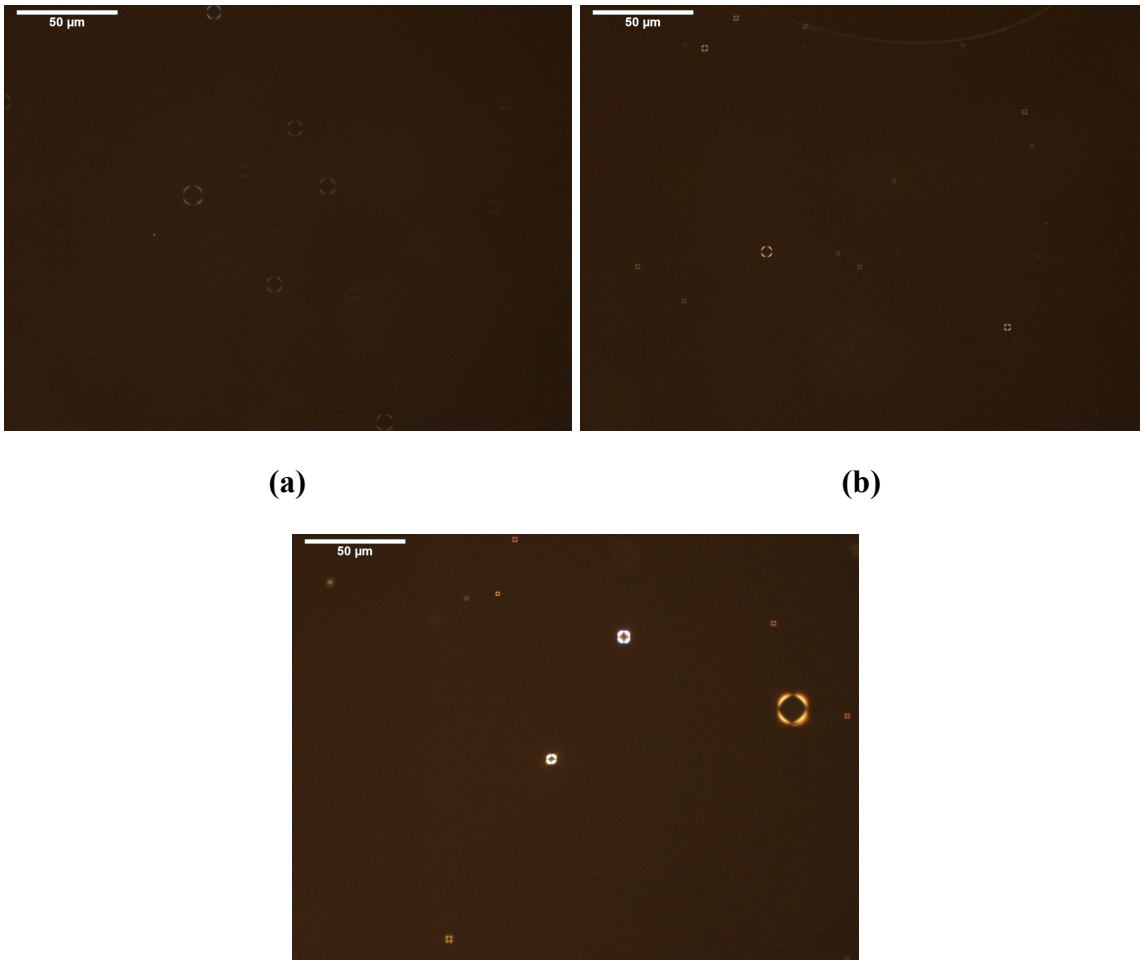

(a) **(b)**

(c)

Figure 4-11 Hydrocarbon droplets showing Maltese cross pattern in water bulk: (a) octane droplets in water bulk; (b) toluene droplets in water bulk; (c) 1-Methylnaphathlene droplets in water bulk.

4.4.3 Curvature of the droplet interface

In Figure 4-12, the shrinking process of DI water droplets on OTS processed slides was recorded using polarized microscopy. It could be seen that the Maltese cross pattern continued existing and the brightness of the pattern almost kept the same as the droplet shrinks. The shrinking occurred naturally as water evaporated. The three images were taken at a time step of 10 seconds.

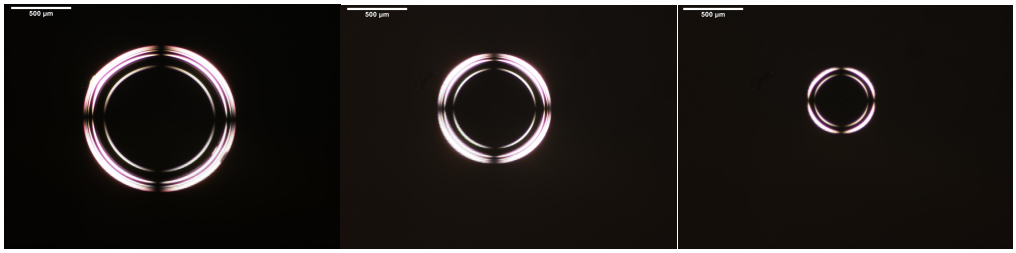

(a) t = 0 **(b) t = 10 seconds** **(c) t = 20 seconds**

Figure 4-12 Microscopic observation of DI water droplet sitting on OTS processed slides under polarized light.

Figure 4-13 presents the comparison of an old droplet (have sat on the slide for 20 seconds) and a new droplet. The two droplets were created by a syringe, using the same amount of water; thus the original sizes of the two droplets were the same.

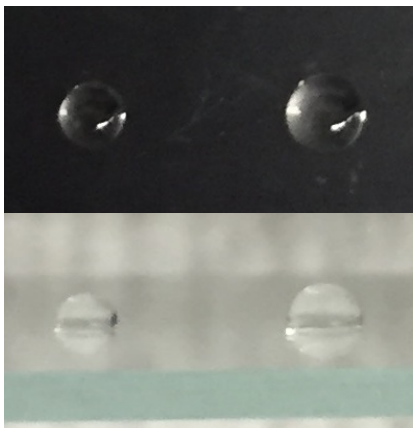

Figure 4-13 Photo of water droplets sitting on OTS processed slides.

Basing on the experiment results, the schematics in Figure 4-14 are drawn to help illustrate the shrinking process of a water droplet sitting on OTS processed slides. As the water evaporated, the size of the water droplet decreases while the contact angle with the surface stayed constant.

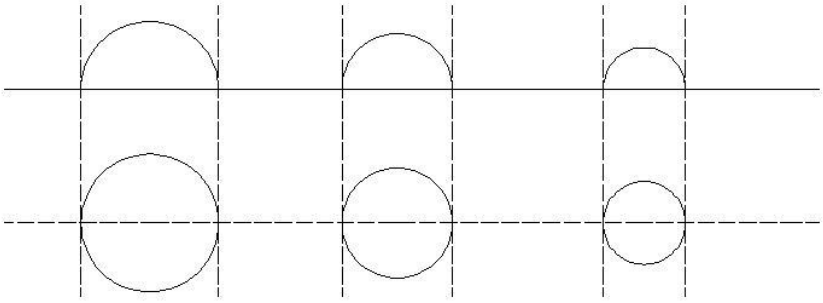

Figure 4-14 Schematic diagram of the shrinking process of water droplets on OTS processed slides.

The same experimental procedure was applied to a water droplet sitting on unprocessed slides, and the results are shown in Figure 4-15, Figure 4-16, and Figure 4-17. In this experiment, images under polarized light were taken at a time step of 2 seconds (see Figure 4-15), and the time interval between new and old droplets is 6 seconds (see Figure 4-17). The schematics in Figure 4-18 illustrate the shrinking process of water droplet sitting on unprocessed slides. As the water evaporates, the curvature of the droplet decreases while the cross-sectional area stays the same. The brightness of the Maltese cross pattern fades gradually with water evaporation. At t = 6 seconds, the Maltese cross pattern disappears under polarized light but the water droplet can still be observed under normal light, as shown in Figure 4-16.

By combining the results of the above two experiments, the curvature of the water surface is a crucial factor that leads to the appearance of the Maltese cross pattern. It is a qualitative experiment. The quantitative relationship between the curvature and the disappearance of the Maltese cross pattern is not detected here.

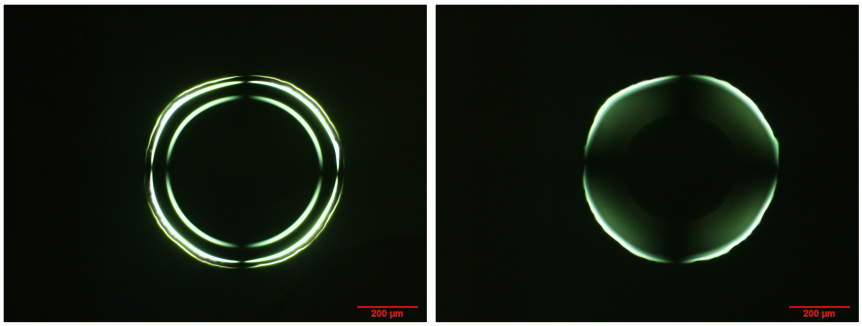

(a) t = 0 seconds **(b) t = 2 seconds**

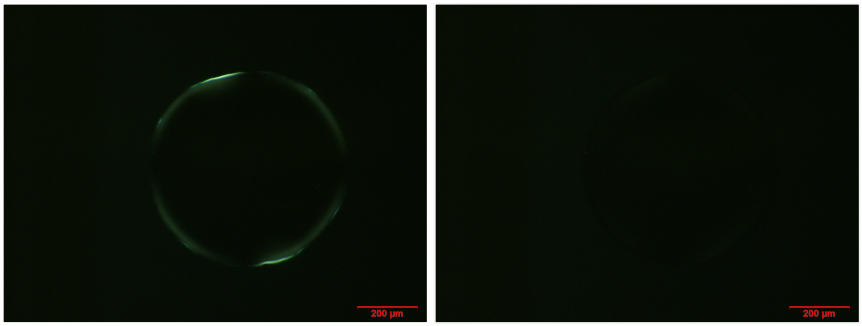

(c) t = 4 seconds **(d) t = 6 seconds**

Figure 4-15 Microscopic observation of DI water droplet sitting on unprocessed slides under polarized light.

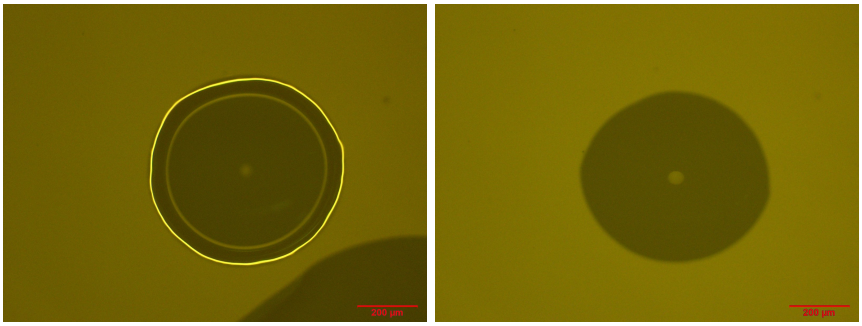

(a) t = 0 **(b) t = 6 seconds**

Figure 4-16 Microscopic observation of DI water droplet sitting on unprocessed slides under normal light.

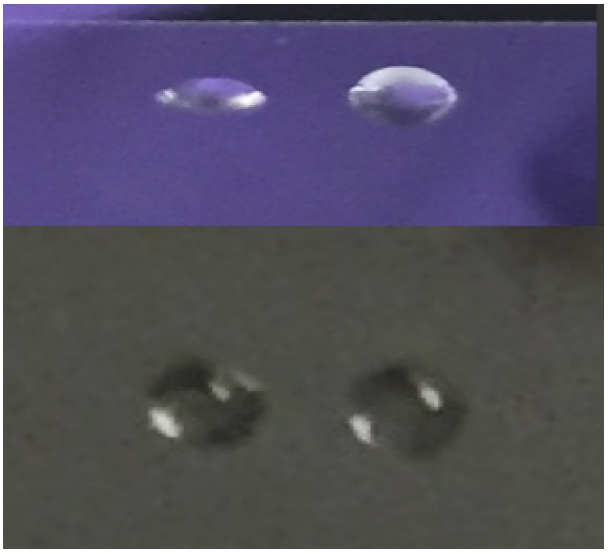

Figure 4-17 Photo of DI water droplets sitting on OTS processed slides.

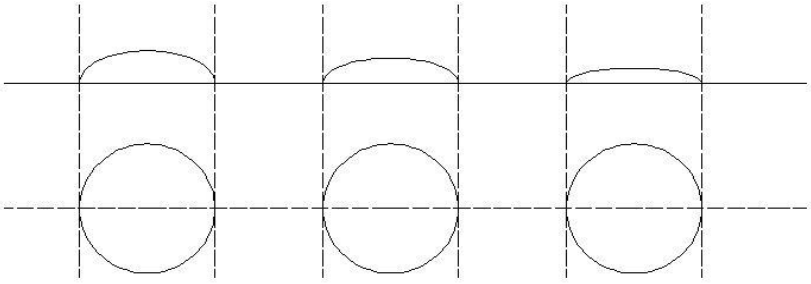

Figure 4-18 Schematic diagram of the shrinking process of DI water on unprocessed slides.

4.4.4 Summary

When working with hydrocarbon-water systems, researchers should take caution to illustrate the appearance of liquid crystals by the criterion of the Maltese cross pattern. Multiple factors, such as light interference among hydrocarbon droplets in water bulk, differences of refractive index between hydrocarbon and water, and the curvature of

water interface, can lead to the appearance of Maltese cross pattern. These factors may apply singly or in combination. Therefore, other properties of liquid crystals must be taken into consideration to help eliminate artifacts when dealing with hydrocarbon-water systems. In section 4.5, control experiments were used to help eliminate the interference of optical artifacts discussed above.

4.5 Formation of liquid crystal layers by humic acids at water/hydrocarbon and water/water interfaces

4.5.1 Hydrocarbon-external-water structure

For sample 6, as seen in Figure 4-19 (a), the solid octacosane particles assemble group by group during the centrifugation. After being heated to melting point and cooled down to room temperature, the solid spherules melted and merged with each other, as a result, large pieces of solids were observed (see image b of Figure 4-19). As for sample 5, with the participation of humic acids, Maltese cross patterns were observed and the patterns did not disappear after being heated over the melting point of octacosane (see Figure 4-20). The size of the spherules showing the Maltese cross pattern can be as large as 8 μm to 10 μm. Figure 4-21 presents the results of the HAs-water system (sample 7). It shows fewer Maltese patterns and the size of the patterns is also smaller - 3 μm to 4 μm. The formation of lyotropic liquid crystals in humic acid-water systems was discussed in Chapter 4.3. Considering the amphiphilic properties of humic acid, lyotropic liquid crystalline phases can also be formed by molecule aggregation surrounding a hydrocarbon droplet [64] in a ternary water-surfactant-hydrocarbon system. Multiple

cases of liquid crystal formation by different surfactants have been reported [65 - 67]. Researchers have also presented and illustrated biplex structures of liquid crystals with an isotropic inner core could show Maltese cross patterns [1, 14, 29]. Masik [14] illustrated biplex structures using a conceptual schematic, reproduced as Figure 4-22, and demonstrated it by using depth profiling. The octacosane particles of sample A did not merge with each other during the process of heating and the biplex liquid crystal structure persisted. This is because the outer shell composed of liquid crystals works as a wall to inhibit the fusion of particles. Our result agrees well with the experiments reported by Liu & Friberg [7] and Horvath-Szabo´ [31]. They reported that liquid crystals tend to be located at the oil-water interface of the droplets and hinder the coalescence of droplets in emulsions. In addition, ring patterns were also observed in the sample from the octacosane-HAs-water system, as presented in Figure 4-23. The size of the bright rings with a dark core can be as large as 20 μm. The bright outer layer is much thicker than that of spherules showing the Maltese cross pattern. Under polarized light, the ring patterns coexist with the Maltese cross patterns. They are actually the same structure under normal light. Thus, the large ring structures provide direct evidence of the formation of biplex structures. It is assumed that the organization of liquid crystals on the outer layer and the large thickness lead to intense light illumination, which covers the dark parts of the Maltese cross. This speculation can be verified by Figure 4-24, which was obtained from image (a) of Figure 4-23 by adjusting its contrast to 42.1 and brightness to 15, and then Sobel boundary detection was applied. The image was processed by software Stream Essentials. Figure 4-24 reveals that the essence of a large ring pattern is the same with the Maltese cross pattern.

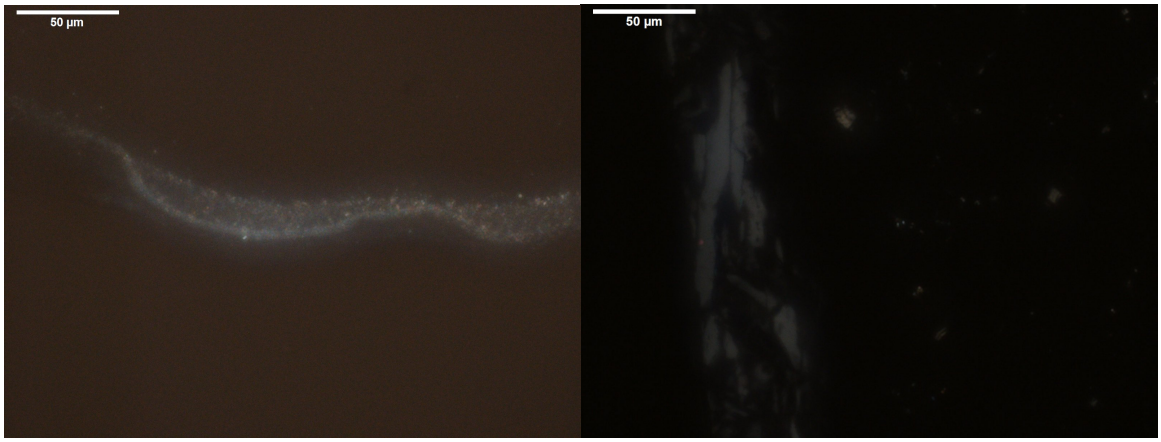

(a) **(b)**

Figure 4-19 Octacosane-water mixture under polarized light: (a) octacosane particles after centrifugation; (b) ocatacosane particles after being heated and cooled down.

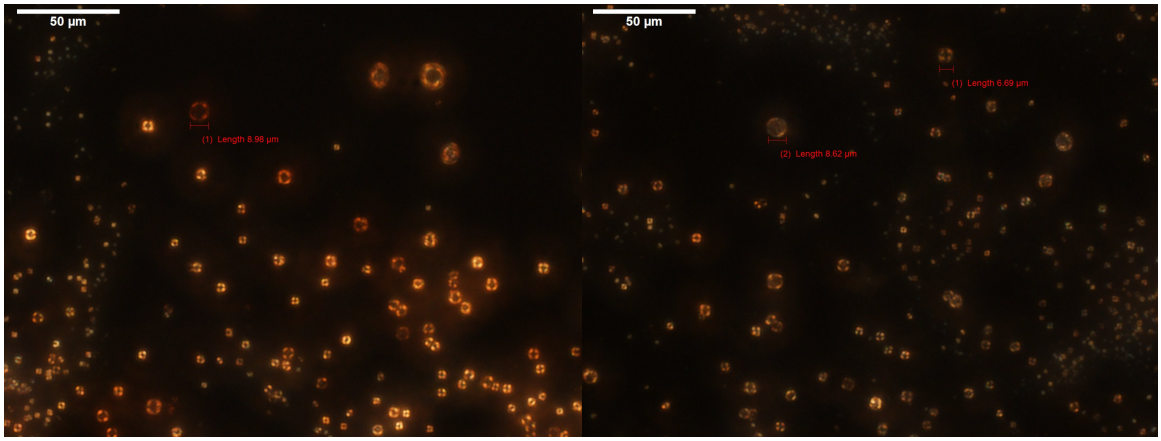

(a) **(b)**

Figure 4-20 Octacosane-HAs-water mixture under polarized light: (a) liquid crystal coated particles before being heated; (b) liquid crystal coated particles after being heated and cooled down.

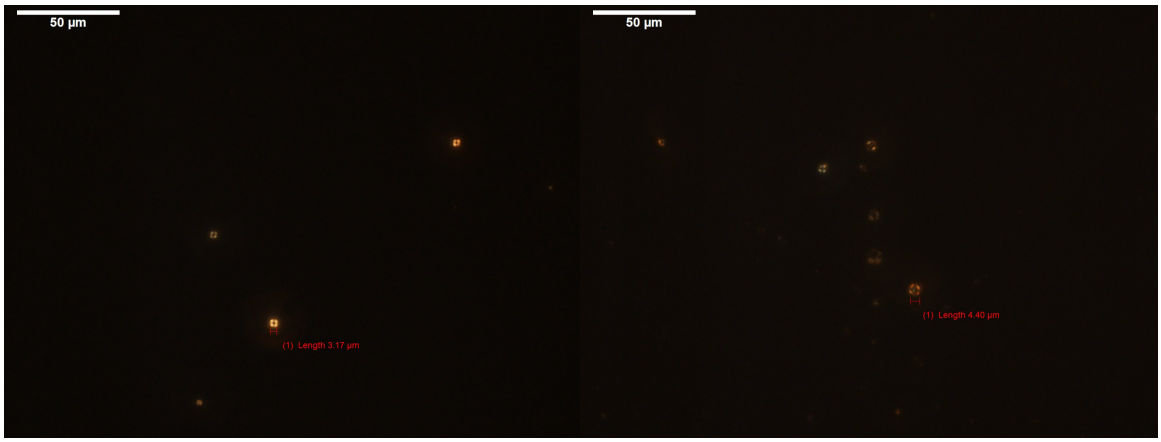

(a) **(b)**

Figure 4-21 HAs-water system under polarized light: (a) water evaporated; (b) after being heated and cooled down.

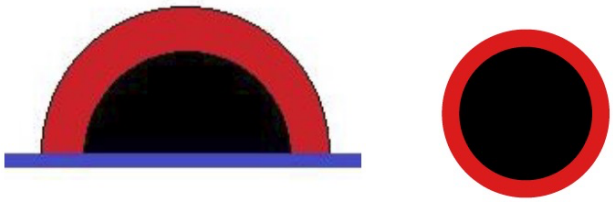

Figure 4-22 Left: a cross-sectional view of a liquid crystal domain on a surface; right: Bottom-up/top-down view of a liquid crystal domain on a surface. [14]

The result of sample 8 (5CB-HAs-water system) is presented in Figure 4-25. Biplex liquid crystal structures were also observed, and the structure remained intact during heating sample 5. The behavior of samples 8 and 5 are similar to the results reported by Qin [29] and Duncke et al. [33], presented in Figure 4-26 and Figure 4-27. Qin [20] observed biplex liquid crystals when trying to extract liquid crystals from bitumen to water and Duncke et al. [33] observed biplex liquid crystals in crude oil emulsion fractions. These prior works are examples of hydrocarbon-liquid crystal-water systems.

Taken together with results from the peer-reviewed literature, it is clear that the octacosane-HA-Water system exhibits biplex-structured liquid crystals.

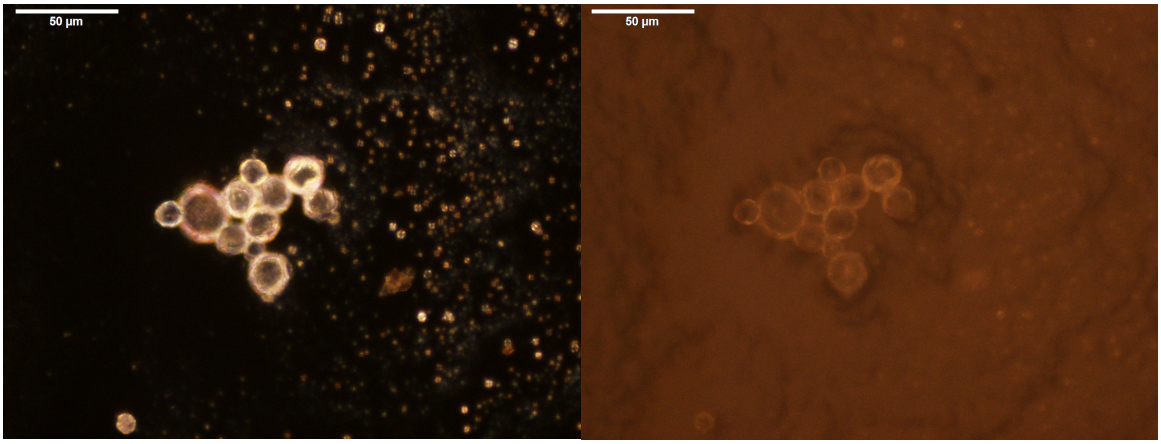

(a) **(b)**

Figure 4-23 Octacosane-HAs-water system after water evaporated: (a) under polarized light; (b) under normal light.

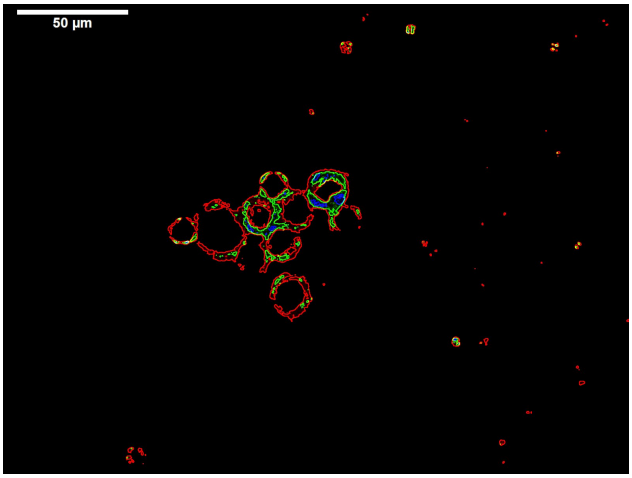

Figure 4-24 Octacosane-HAs-water system after water evaporated: Sobel boundary detection applied.

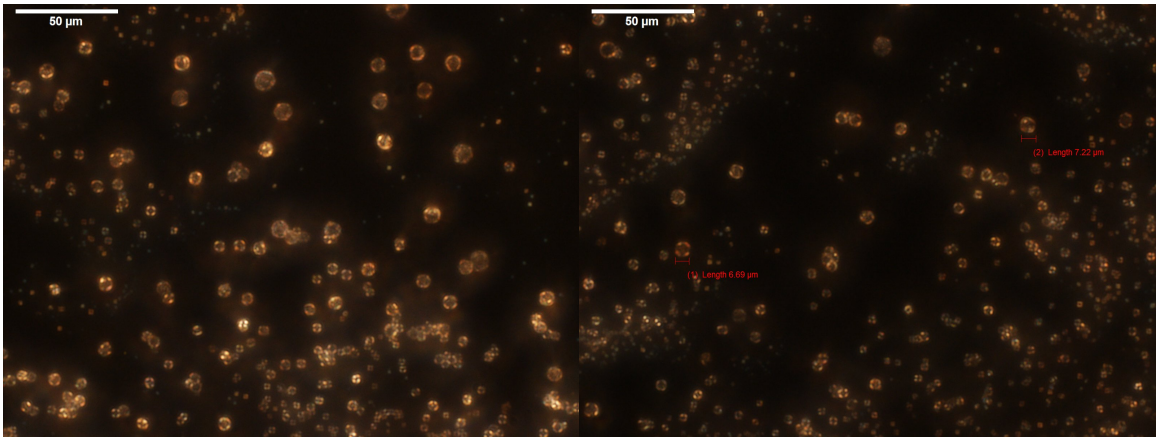

(a) **(b)**

Figure 4-25 Octacosane-5CB-water mixture under polarized light: (a) 5CB coated particles before being heated; (b) 5CB coated particles after being heated and cooled down.

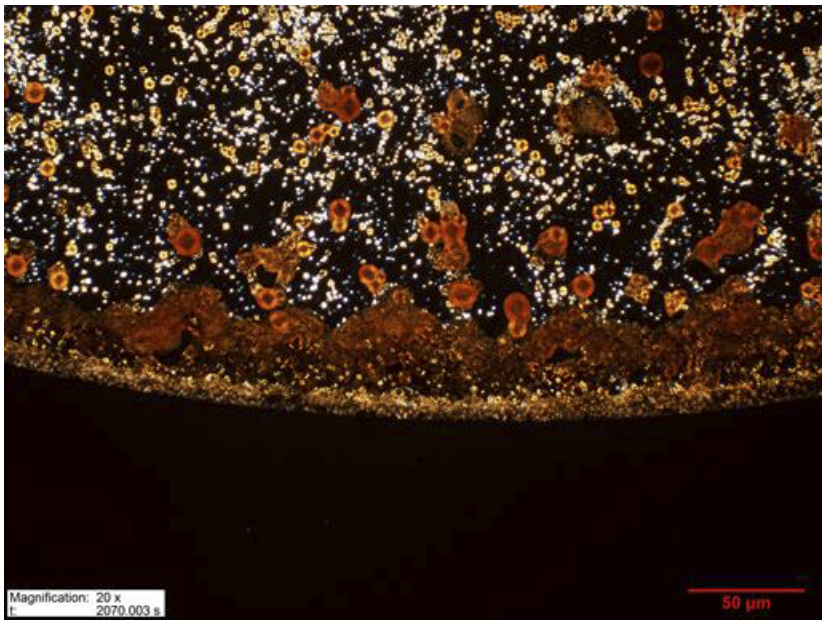

Figure 4-26 Liquid crystal domains transferred from bitumen to water. [29]

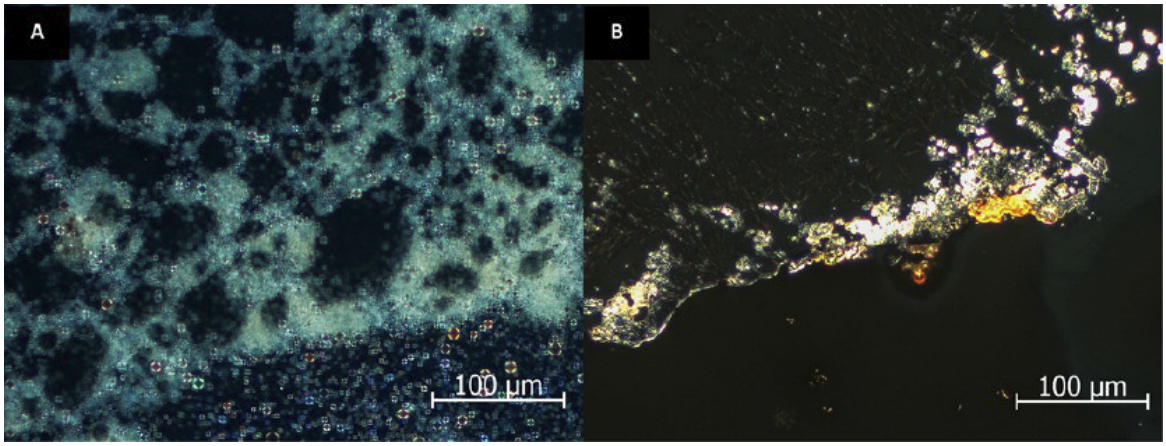

Figure 4-27 Liquid crystal domains in emulsion fractions from crude oil, during (a) and (b) after water evaporation. [33]

4.5.2 Water-external-water structure

Figure 4-28 shows an image of sample 9 captured before water evaporated under polarized light. Maltese cross patterns can be observed, and the size of the crosses can reach as large as 50 µm. Particles of naphthalene coexist with the Maltese crosses. Figure 4-29 presents a process of droplet bursting. Droplets in Figure 4-28 are the same ones as those showing Maltese crosses in Figure 4-29. The droplets' positions do not match exactly in these two figures because the droplets keep moving in the bulk water. As the bursting process occurs in a short time, it is not allowed to switch between polarized light and normal light. It is clearly presented in Figure 4-29 that the inner material restrained inside the liquid crystal layer is liquid. As the only liquid species in sample 9 is water, it is sound to assume that the droplets in bulk water correspond to the water-external-water structure. The layer bounds the water droplets showing the Maltese cross pattern is comprised of liquid crystals stemming from humic acids. The water-external-water

structure is not stable when sitting on slides and it bursts out as the bulk water evaporates. In addition, bright ring structures were observed in the 5CB-water system (sample 12) and highly concentrated water-HAs-Naphthalene system (sample 13), as presented in Figure 4-30. The HAs concentration in sample 13 is five times of that in sample 9. The size of the ring in the 5CB-water system can reach around 50 μm and its isotropic inner core presenting dark under polarized light. Therefore, the ring here should be a water-liquid crystal-water structure. The rings observed in sample 13 present the exactly same structure with that of the 5CB-water system, which lends the confidence to believe that water-liquid crystal-water structure is also formed in the water-HAs-Naphthalene system. Whether naphthalene is involved in comprising the liquid crystal layer is unknown and needs further exploration.

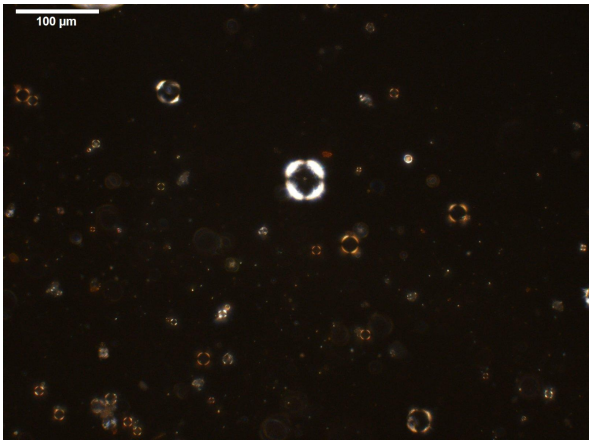

Figure 4-28 Water-external-water structure showing Maltese cross patterns under polarized light.

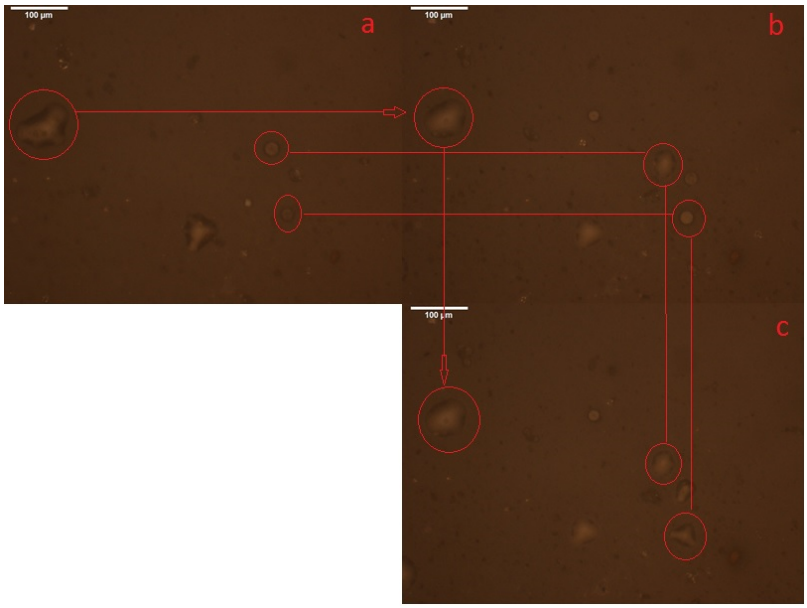

Figure 4-29 Water-external-water structure bursting out as water evaporating, under normal light.

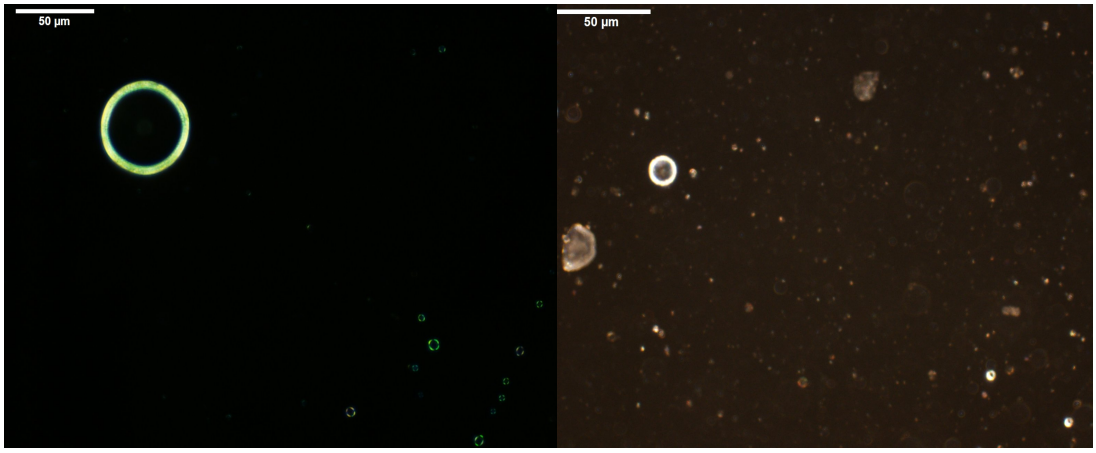

(a) **(b)**

Figure 4-30 Water-liquid crystal-water structure under polarized light: (a) ring structure in the 5CB-water system; (b) ring structure in the water-HAs-naphthalene system.

A process of droplet collapse under polarized light was also recorded (see Figure 4-31). As the bulk water evaporates, the environment supporting the water-liquid crystal-water structure is impaired, leading to the collapse of the droplet. During the collapse process, the birefringent liquid crystals on the droplet surface can be observed.

Results of sample 10 and 11 are presented in Figure 4-32 and Figure 4-33, respectively. Sample 10 and 11 are designed as controls. Naphthalene solid particles are shown in Figure 4-32, and liquid crystal droplets formed by humic acids in water can be observed in Figure 4-33. The biplex structure that appears as large Maltese crosses and the bursting or collapse process are not observed neither in the humic acids-water system nor in the naphthalene-water system. By comparing the results of the five samples comprehensively, it is evident that the water-external-water structure can be formed in the water-HAs-naphthalene system.

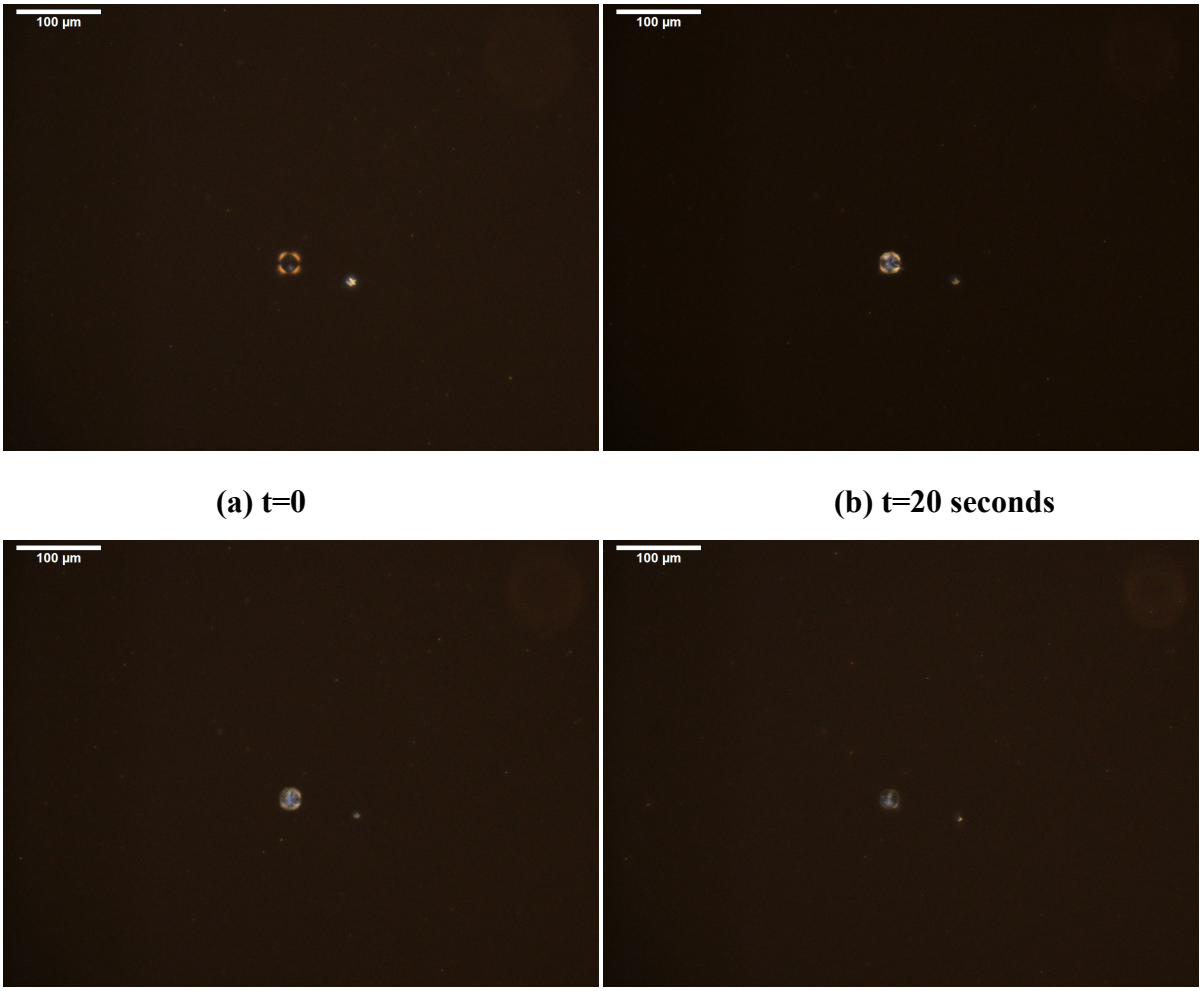

(a) t=0 **(b) t=20 seconds**

(c) t=40 seconds **(d) t= 60seconds**

Figure 4-31 The collapse process of water-extal-water structure under polarized light.

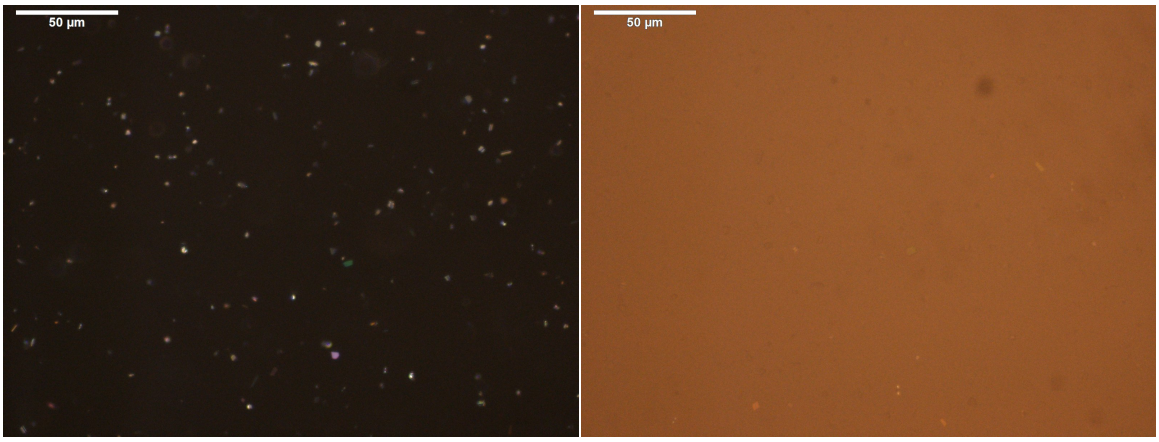

(a) **(b)**

Figure 4-32 Naphthalene particles in dried naphthalene-water mixture: (a) under polarized light; (b) under normal light.

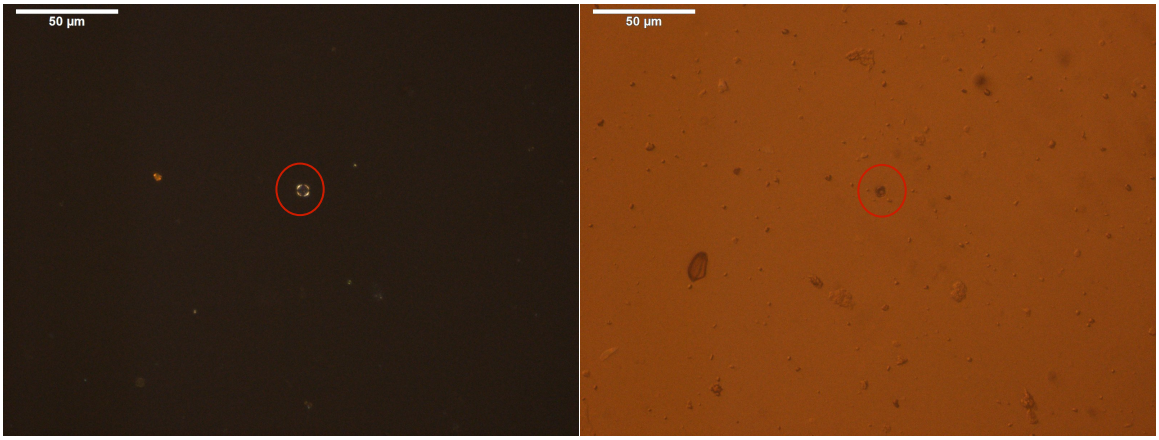

(a) **(b)**

Figure 4-33 Liquid crystals in HAs-water mixture (water evaporated): (a) under polarized light; (b) under normal light.

4.5.3 Water-external-hydrocarbon structure

Figure 4-34 presents the result of the observation of water droplets dispersed in dodecane bulk. Under normal light, the water droplets can be observed clearly. Under polarized light, these water droplets do not show any Maltese cross patterns. Figure 4-35 shows the observation of water-humic acid droplets that are dispersed in dodecane. The droplets show Maltese cross patterns under polarized light, which indicates the existence of liquid crystals at the water-hydrocarbon interface. As shown in Figure 4-36, the inner core of droplets appears green after the water-based coloring agent is involved in the system and the bulk hydrocarbon appears dark. Combing these facts observed, it is sound to say that the water-external-hydrocarbon structure can be created by humic acids; it can form a liquid crystal layer at the interface of water-hydrocarbon emulsion. The result in this experiment agrees well with the reports of Tixier [67] and Ito [68]. They illustrated the creation of W/O type emulsion with liquid crystals located on the interface of the droplets, and the droplets showed Maltese cross pattern under polarized light. The water-HAs-hydrocarbon system in this experiment could keep stable, and the Maltese cross pattern could still be observed after keeping still in room environment for 14 days. However, the system would finally dispel, and the mixture became stratified when observed 60 days later.

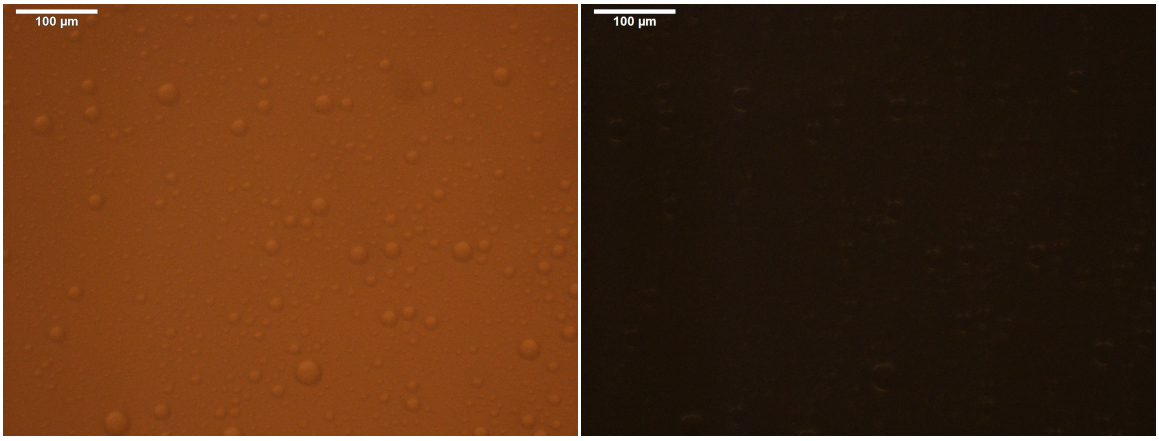

(a) **(b)**

Figure 4-34 Water droplets dispersed in dodecane bulk: (a) under normal light; (b) under polarized light.

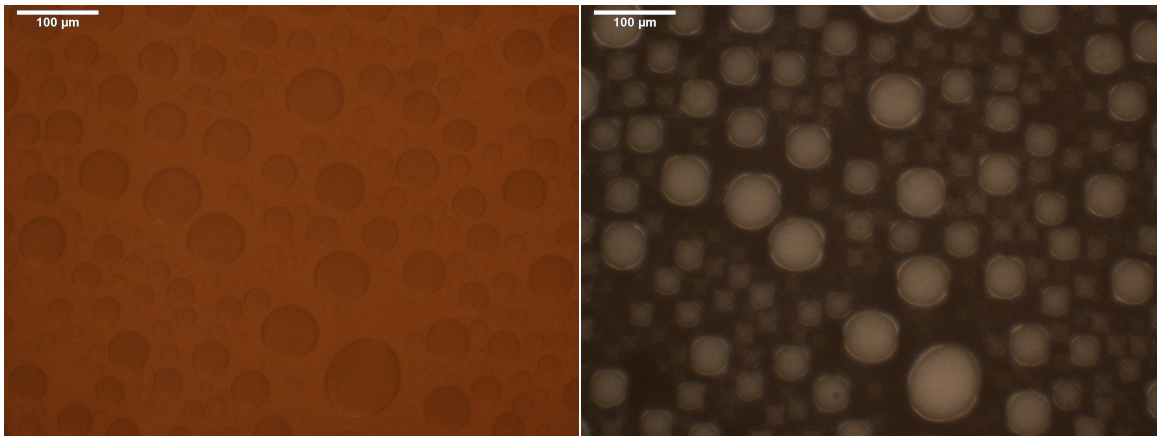

(a) **(b)**

Figure 4-35 HAs dissolved water droplets dispersed in dodecane bulk: (a) under normal light; (b) under polarized light.

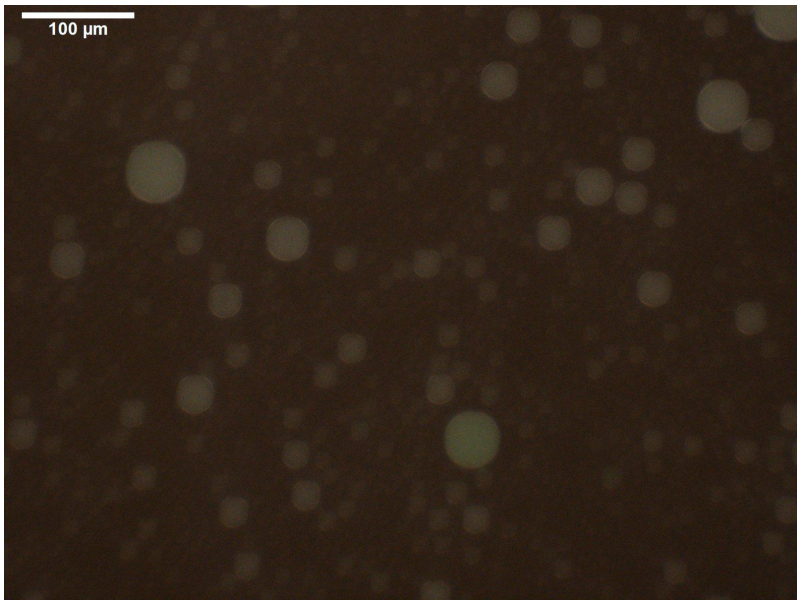

Figure 4-36 Colored water-HAs-dodecane mixture under polarized light.

4.5.4 Summary

Artifacts pose significant challenges for the identification of actual liquid crystalline behaviors in water-hydrocarbon-humic acid systems. Care must be taken to avoid over or miss interpreting experimental results. With the implementation of careful control experiments and with reference to the literature, we were able to demonstrate that water-humic acids-hydrocarbon system verified three types of biplex structures, which are the hydrocarbon-external-water structure, water-external-water structure and water-external-hydrocarbon structure. We were unable to demonstrate the fourth anticipated type of hydrocarbon-HA-hydrocarbon structure set as a goal of this work illustrated in Figure 1-2. Lyotropic liquid crystalline layer formed from humic acids at a concentration higher than its CMC distributes at the interfaces of these biplex structures.

Chapter 5 Conclusions and Future Work

Humic acids, present in groundwater and hydrocarbon resources, were hypothesized to be a source of liquid crystal domains in Athabasca bitumen and other hydrocarbon resources co-produced with water. In this work, we tested this hypothesis, and it shows that three of the four behaviors outlined in Figure 1-2 are replicated. We were unable to illustrate thermotropic liquid crystalline behaviors. Further, we underscored the impact of artifacts in this field of study.

5.1 Specific findings:

- Humic acid, solid at room temperature, does not form thermotropic liquid crystals over the temperature range 296.16 K to 600.16 K. They stay solid phase and partially decompose on heating rather than melting.
- Material extracted from humic acid by anhydrous ethyl alcohol shows liquid crystalline properties at room temperature. The liquid crystal drops present Maltese cross patterns on octadecyltrichlorosilane treated hydrophobic slides and show fan-shaped patterns on hydrophilic slides. The diameter of the liquid crystal domains on hydrophobic slides ranges from 2 μm to 5 μm and the domains can grow to 10 – 20 μm after some time of incubation under ambient conditions. This behavior was discriminated from the behavior of isotropic drops in water. The composition of the liquid crystals was not verified but includes constituents from the humic acid in addition to ethyl alcohol.

- Lyotropic liquid crystal spherules form in unfractionated humic acid-water mixtures when the humic acid concentration exceeds the critical micelle concentration (7g/L). The observed diameter of the liquid crystal spherules was around 2.5 μm to 4.5 μm. The measured number size distribution included droplets as small as 20 nm. The measured size distribution shifted to larger droplets and the distribution broadened, as temperature increases.
- Lyotropic liquid crystal domains with homogeneous hydrocarbon cores and humic substance liquid crystalline shells dispersed in aqueous liquids were created in hydrocarbon-humic acid-water systems. The observed diameter of the domains ranges from 2.5 μm to 20 μm, which is one order of magnitude smaller than those discovered in Athabasca bitumen, but of the same order of magnitude of those reported in water-rich phase, transferred from bitumen.
- Lyotropic liquid crystal domains with homogeneous aqueous cores and humic substance liquid crystalline shells dispersed in aqueous liquids were created.
- Lyotropic liquid crystal domains with homogeneous aqueous cores and humic substance liquid crystalline shells dispersed in hydrocarbon liquids were also created.
- Optical artifacts such as light interference, the difference of refractive index, and interface curvature can lead to the appearance of Maltese cross pattern under polarized light. All the assertions of liquid crystals appearance made in this thesis have taken multiple properties of liquid crystals to eliminate the possibility of optical artifacts.

5.2 Recommendations for Future Work

- The composition of the anhydrous ethyl alcohol extracted humic acid (EHA) should be analyzed in detail, such as with FT-ICR, to compare their elemental composition and molecular structures with liquid crystals isolated from Athabasca bitumen.
- Links with properties of interfacial materials that stabilize water-oil emulsion should be studied.
- Liquid crystals extracted from humic acid may have potential commercial applications worth exploring.
- It is not clear what materials or combinations of materials lead to the formation or apparent formation of thermotropic liquid crystalline behavior. It might be explained by that the temperature change affects the critical concentration needed for humic acid to show lyotropic behavior, but further study is needed.

Reference

1. Bagheri, S.R., et al., *Observation of Liquid Crystals in Heavy Petroleum Fractions* Energy & Fuels, 2010. 24(8): p. 4327-4332.
2. Bagheri, S.R., Masik, B., Arboleda, P., Wen, Q., Michaelian, K.H. and Shaw, J.M., *Physical properties of liquid crystals in Athabasca bitumen fractions*. Energy & fuels, 2012, *26*(8): p.4978-4987.
3. Qin, C., Becerra, M. and Shaw, J.M., *Fate of Organic Liquid-Crystal Domains during Steam-Assisted Gravity Drainage/Cyclic Steam Stimulation Production of Heavy Oils and Bitumen*. Energy & Fuels, *31*(5), 2017, p.4966-4972.
4. Wang, K, On the Separation and Composition of Liquid Crystals in Athabasca Bitumen, 2015, MSc Thesis, University of Alberta.
5. de Gennes, P.G. and J. *Prost, The physics of liquid crystals. 2nd ed. The International Series of Monographs on Physics*, New York: Oxford University Press. 1993, p. 597.
6. Duncke, A.C., et al., *Liquid Crystal Observations in Emulsion Fractions from Brazilian Crude Oils by Polarized Light Microscopy*. Energy & Fuels, 2016, *30*(5): p. 3815-3820.
7. Liu, Y., & Friberg, S.E., *Role of Liquid Crystal In the Emulsification of A Gel Emulsion With High Internal Phase Fraction*. Journal of colloid and interface science, 2009, *340*(2): p. 261-268.
8. Urdahl, O. and Sjöblom, J., *Water-in-crude oil emulsions from the Norwegian Continental Shelf. A stabilization and destabilization study*. Journal of dispersion science and technology, 1995, *16*(7), p.557-574.
9. Laughlin, R.G., 1994. *The aqueous phase behavior of surfactants* (Vol. 6). Academic Press.
10. Friberg, S., Mandell, L. and Larsson, M., *Mesomorphous phases, a factor of importance for the properties of emulsions.* Journal of Colloid and Interface Science, 1969, *29*(1), p.155-156.
11. Friberg, S. and Rydhag, L., *The system: Water-p-xylene-l-aminooctane-octanoic acid*. Kolloid-Zeitschrift und Zeitschrift für Polymere, 1971, *244*(1), p.233-239.
12. Kavaliunas, D.R. and Frank, S.G., *Liquid crystal stabilization of multiple emulsions.* Journal of Colloid and Interface Science, 1978, *66*(3), p.586-588.
13. . Friberg, J. and Mandell, L., *Influence of phase equilibria on properties of emulsions*. Journal of pharmaceutical sciences, 1970, *59*(7), p.1001-1004.
14. Masik, B.K., Separation and analysis of liquid crystalline material from heavy petroleum fractions, in Department of Chemical and Materials Engineering 2011, University of Alberta: Edmonton.
15. Xu, Y., Dabros, T., Hamza, H. and Shefantook, W., *Destabilization of water in bitumen emulsion by washing with water*. Petroleum science and technology, 1999, *17*(9-10), p.1051-1070.
16. Young, C. and von Wandruszka, R., *A comparison of aggregation behavior in aqueous humic acids*. Geochemical Transactions, 2001, *2*(2), p.16-20.
17. Gutierrez, L. and Pawlik, M., 2014. Influence of humic acids on oil sand processing. Part I: Detection and quantification of humic acids in oil sand ores

and their effect on bitumen wettability. *International Journal of Mineral Processing*, *126*, pp.117-125.
18. Laplante, Michelle. An investigation of the interactions between organic contaminants and various humic acids by DSC analysis. Diss. University of Calgary, 1998.
19. Neto, Antônio M. Figueiredo, and Silvio RA Salinas. The physics of lyotropic liquid crystals: phase transitions and structural properties. Vol. 62. OUP Oxford, 2005.p1
20. Liquid crystal-Ordering. [cited 2017, Nov 23rd]; Available from: http://photonicswiki.org/index.php?title=File:LiquidCrystal-Ordering.jpg
21. Neto, Antônio M. Figueiredo, and Silvio RA Salinas. The physics of lyotropic liquid crystals: phase transitions and structural properties. Vol. 62. OUP Oxford, 2005, p. 2.
22. Lipid bilayer and micelle. [cited 2017, Nov 23rd]; Available from: https://commons.wikimedia.org/wiki/File:Lipid_bilayer_and_micelle.png
23. Brown, G.H. and W.G. Shaw, *The Mesomorphic State - Liquid Crystals*. Chemical Reviews, 1957. **57**(6): p. 1049-1157.
24. Syrbu, S., R.Y. Golovanov, and V. Klopov, *Properties of Some Mesogens in the Liquid Crystal and Isotropic States.* Theoretical Foundations of Chemical Engineering, 2003. 37(2): p. 204-206.
25. *Introduction to liquid crystals*. [cited 2017, Nov 23rd]; Available from: http://barrett-group.mcgill.ca/teaching/liquid_crystal/LC02.htm.
26. Scharf, Toralf. Polarized light in liquid crystals and polymers. John Wiley & Sons, 2007. p. 150.
27. Hu, Q. Z., and Jang, C. H., *Spontaneous Formation of Micrometer-scale Liquid Crystal Droplet Patterns on Solid Surfaces and their Sensing Applications*. Soft Matter, 2013. *9*(24): p.5779-5784.
28. Smectic A - Nematic phase transition. 2004 [cited 2018 July 5]; Available from: http://commons.wikimedia.org/wiki/File:Smectic nematic.jpg.
29. Qin, Chuan. On organic liquid crystal transfer from bitumen-rich to water-rich phases: A combined laboratory and SAGD field study. Diss. University of Alberta, 2014.
30. Scharf, Toralf. Polarized light in liquid crystals and polymers. John Wiley & Sons, 2007. p. 4.
31. Horváth Szabó, G., Masliyah, J.H. and Czarnecki, J., 2006. *Friberg correlations in oil recovery*. Journal of dispersion science and technology, 27(5), p.625-633.
32. Scharf, Toralf. Polarized light in liquid crystals and polymers. John Wiley & Sons, 2007. p. 55.
33. Duncke, A. C., Marinho, T. O., Barbato, C. N., Freitas, G. B., de Oliveira, M. C., & Nele, M. (2016). *Liquid Crystal Observations in Emulsion Fractions from Brazilian Crude Oils by Polarized Light Microscopy*. Energy & Fuels, 30(5), 3815-3820.
34. Czarnecki, J., *Stabilization of Water in Crude Oil Emulsions*. Part 2. Energy & Fuels, 2009. 23: p. 1253-1257.
35. James A. Rice and Patrick MacCarthy. *Statistical evaluation of the elemental composition of humic substances*. Org. Geochem. 1991, 17(5): p. 635-648

36. Bazyleva, A.B., et al., *Bitumen and Heavy Oil Rheological Properties: Reconciliation with Viscosity Measurements*. Journal of Chemical & Engineering Data, 2009. 55(3): p. 1389-1397.
37. John V. Headley and Dena W. McMartin. *A Review of the Occurrence and Fate of Naphthenic Acids in Aquatic Environments*. Journal of environmental science and health Part A—Toxic/Hazardous Substances & Environmental Engineering. 2004, A39(8): p. 1989-2010.
38. Pettit R E. Organic matter, humus, humate, humic acid, fulvic acid and humin: their importance in soil fertility and plant health. 2004 [cited 2017, Nov 23rd]; Available from: www.humate.info/mainpage.htm.
39. Donald F. Smith, Tanner M. Schaub, Sunghwan Kim, Ryan P. Rodgers, Parviz Rahimi, Alem Teclemariam, and Alan G. *Marshall.Characterization of Acidic Species in Athabasca Bitumen and Bitumen Heavy Vacuum Gas Oil by Negative-Ion ESI FT-ICR MS with and without Acid-Ion Exchange Resin Prefractionation*. Energy & Fuels, 2008, 22: p. 2372-2378
40. MacCarthy, P., *The principles of humic substances*. Soil Science, 2001, 166 (11), p.738-751.
41. Sparks, D.L., *Chemistry of soil organic matter*. Environmental soil chemistry, 2003, p.75-113.
42. Stevenson, F.J., 1994. *Humus chemistry: genesis, composition, reactions*. John Wiley & Sons.
43. Guetzloff, T. F., & Rice, J. A., *Does humic acid form a micelle?*. Science of the total environment. 1994, 152(1), p. 31-35.
44. Guetzloff, T.F. and Rice, J.A., 1996. *Micellar nature of humic colloids*. p. 18-25.
45. Neto, Antônio M. Figueiredo, and Silvio RA Salinas. *The physics of lyotropic liquid crystals: phase transitions and structural properties*. Vol. 62. OUP Oxford, 2005, p9.
46. Zetasizer Nano Z Brochure. [cited 2017 October 15]; Available from https://www.malvern.com/en/products/product-range/zetasizer-range/zetasizer-nano-range/zetasizer-nano-z/
47. Introduction to dynamic light scattering. [cited 2017 October 15]; Available from https://en.wikipedia.org/wiki/Dynamic_light_scattering#/media/File:DLS.svg
48. Scharf, Toralf. Polarized light in liquid crystals and polymers. John Wiley & Sons, 2007. P4
49. Refractive index database. [cited 2017 November 3]; Available from https://refractiveindex.info/?shelf=organic&book=toluene&page=Kedenburg
50. Gallo, R., Ricca, G. and Severini, F., *Thermal Behaviour of Fulvic and Humic acids in Comparison with a Maleic Anhydride Oligomer*. Thermochimica Acta, 1991. *182*(1): p.1-7.
51. Krishna, K.V., and Verma, S., *Investigating the Avidin-Biotin Interaction on Chiral Soft Structure Platforms*. Australian Journal of Chemistry, 2011. *64*(5): p. 576-582.
52. Jákli, A., et al., *Optically Induced Periodic Structures in Smectic-C Liquid Crystals*. Physical Review E, 2000, *63*(1): p. 011705.

53. Xia, Y., Serra, F., Kamien, R. D., Stebe, K. J., & Yang, S. *Direct Mapping of Local Director Field of Nematic Liquid Crystals at the Nanoscale*. Proceedings of the National Academy of Sciences, 2015, *112*(50), p. 15291-15296.
54. Miyajima, D., et al., *Columnar Liquid Crystal With a Spontaneous Polarization Along the Columnar Axis.* Journal of the American Chemical Society, 2010. *132*(25): p. 8530-8531.
55. Weissflog, W., Lischka, C. H., Diele, S., Wirth, I., & Pelzl, G., *The Inverse Phase Sequence SmA-SmC in Symmetric Dimeric Liquid Crystals.* Liquid Crystals, 2000. *27*(1): p. 43-50.
56. Reizlein, K., and Hoffmann, H., *New Lyotropic Nematic Liquid Crystals.* Progress in Colloid & Polymer Science, 1984: p. 83-93.
57. Donald, AM and Windle, A.H., *Liquid Crystalline Polymers*. 1992, Cambridge: Cambridge University Press.
58. Angel, M., et al., *From Rodlike Micelles to Lyotropic Liquid Crystals*. Progress in Colloid & Polymer Science, 1984: p. 12-28.
59. Redkar, M., Hassan, P. A., Aswal, V., & Devarajan, P., *Onion Phases of PEG-8 Distearate*. Journal of pharmaceutical sciences, 2007, *96*(9): p. 2436-2445.
60. Akpinar, E., Reis, D., Yildirim, M., & Neto, A. M. F., (2014). *New Lyotropic Mixtures with Non-chiral N-acylamino Acid Surfactants Presenting the Biaxial Nematic Phase Investigated by Laser Conoscopy, Polarized Optical Microscopy and X-ray Diffraction*. Materials, 2014, *7*(6): p. 4132-4147.
61. Horváth-Szabó, G., Czarnecki, J., & Masliyah, J., *Liquid Crystals in Aqueous Solutions of Sodium Naphthenates.* Journal of Colloid and Interface Science, 2001, *236*(2): p. 233-241
62. Syamala, P.P., Soberats, B., Görl, D., Gekle, S. and Würthner, F. *Thermodynamic insights into the entropically driven self-assembly of amphiphilic dyes in water.* Chemical Science, 2019, *10*(40): p.9358-9366.
63. Nicoli, D.F., et al., *High-resolution Particle size Analysis of Mostly Submicrometer Dispersions and Emulsions by Simultaneous Combination of Dynamic Light Scattering and Single-particle Optical Sensing*. American Chemical Society, 1998: p 52-76.
64. Rodriguez-Abreu, C., Acharya, D.P., Aramaki, K., and Kunieda, H., *Structure and Rheology of Direct and Reverse Liquid-crystal Phases in A Block Copolymer/water/oil System.* Colloids and Surfaces A: Physicochemical and Engineering Aspects, 2005, *269*(1-3): p. 59-66.
65. Frank, C., Sottmann, T., Stubenrauch, C., Allgaier, J., & Strey, R. *Influence of Amphiphilic Block Copolymers on Lyotropic Liquid Crystals in Water− Oil− Surfactant Systems.* Langmuir, 2005, *21*(20): p. 9058-9067.
66. Auvray, X., et al., *Influence of Solvent-headgroup Interactions on the Formation of Lyotropic Liquid Crystal Phases of Surfactants in Water and Nonaqueous Protic and Aprotic solvents*. Langmuir, 1992, *8*(11): p. 2671-2679.
67. Tixier, T., Heppenstall-Butler, M., and Terentjev, E.M. *Stability of Cellulose Lyotropic Liquid Crystal Emulsions.* The European Physical Journal E, 2005, 18(4): p. 417-423.

68. Ito, T., Tsuji, Y., Aramaki, K., and Tonooka, N., *Two-step Emulsification Process For Water-in-oil-in-water Multiple Emulsions Stabilized by Lamellar Liquid Crystals*. Journal of oleo science, 2012, *61*(8): p. 413-420.
69. Laštovka, V., Fulem, M., Becerra, M. and Shaw, J.M., *A similarity variable for estimating the heat capacity of solid organic compounds: Part II. Application: Heat capacity calculation for ill-defined organic solids.* Fluid Phase Equilibria, 2008, 268(1-2): p. 134-141.

Appendix I

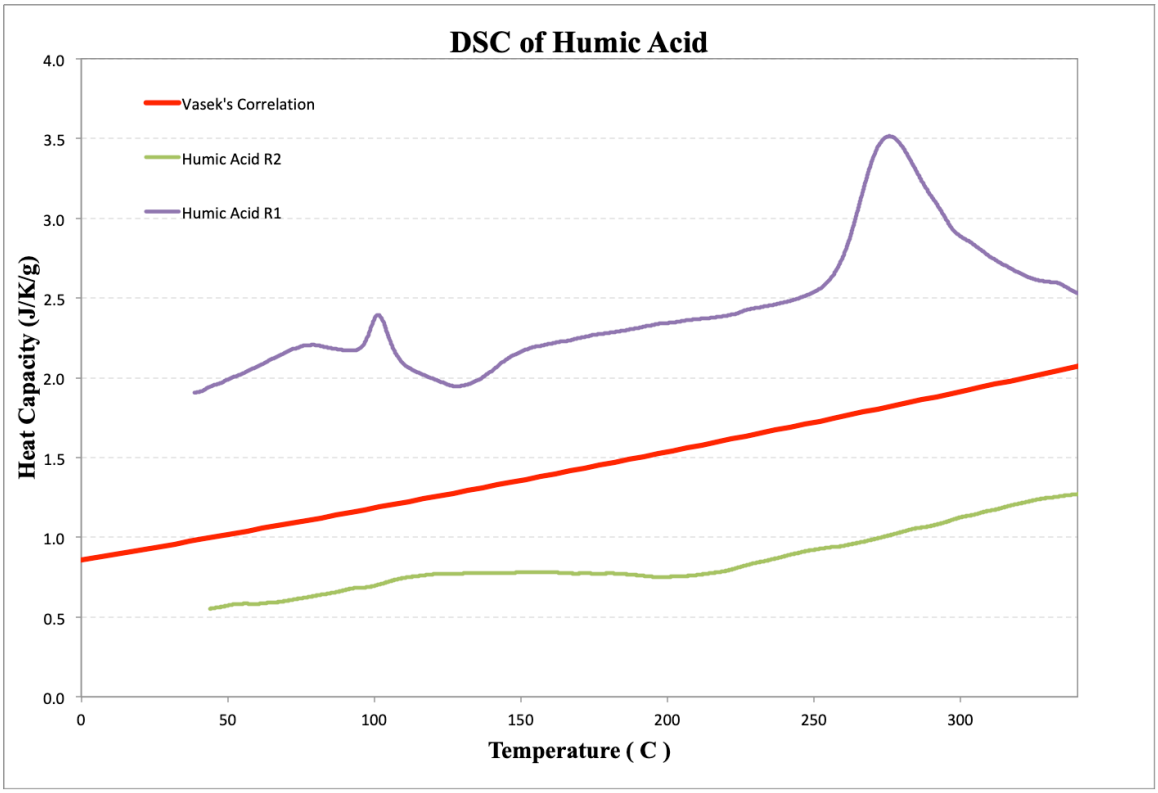

Fgiure A-1 The DSC analysis of humic acid: R1 is the first run of heating; R2 is the second run of heating after cooling down of R1; Vasek's correlation means the heat capacity is calculated using the method provided by Laˇstovka et al. [69].